This is to certify that the

thesis entitled

Characterization of Several Cyclooxygenase Active Site Mutants of Ovine Prostaglandin Endoperoxide H Synthase-1

presented by

Karen Margaret Lakkides

has been accepted towards fulfillment
of the requirements for

M.S. degree in Biochemistry

William L. Smith

Major professor

Date 5/10/00

CHARACTERIZATION OF SEVERAL CYCLOOXYGENASE ACTIVE SITE MUTANTS OF OVINE PROSTAGLANDIN ENDOPEROXIDE H SYNTHASE-1

By

Karen Margaret Lakkides

A THESIS

Submitted to
Michigan State University
in partial fulfillment of the requirements
for the degree of

MASTER OF SCIENCE

Department of Biochemistry

2000

ABSTRACT

CHARACTERIZATION OF SEVERAL CYCLOOXYGENASE ACTIVE SITE MUTANTS OF OVINE PROSTAGLANDIN H SYNTHASE-1

By

Karen Margaret Lakkides

Prostaglandin endoperoxide H synthase (PGHS), which catalyzes the first and committed step in prostaglandin synthesis, exhibits both a cyclooxygenase and a peroxidase activity. The cyclooxygenase active site is involved in converting the substrate, arachidonic acid, to PGG_2. Several residues that are in the ovine PGHS-1 cyclooxygenase active site were investigated using site-directed mutagenesis, including Trp387, Leu384, Met522, and Phe518, which are positioned to have possible roles in maintaining the conformation of substrate during formation of PGG_2, and Gly533, which is positioned to interact with the ω-end of the substrate in the active site.

We determined that Trp387, Leu384, Met522, and Phe518, while not essential for catalysis in oPGHS-1, help maintain the optimal conformation of substrate in the cyclooxygenase active site. Mutations to Trp387 altered the proportions of dihydroxy and monohydroxy products, presumably by changing the spatial constraints necessary to form the kink in the C-9 to C-11 region of arachidonic acid. We also determined that the Gly533 change to an alanine mutant resulted in a loss of all cyclooxygenase activity, probably due to spatial constraints of the ω-end of the substrate that are critical to the positioning of substrate in the active site.

ACKNOWLEDGMENTS

I would first like to thank Dr. William Smith for all of his guidance and support while I have been in his laboratory. He was immensely helpful in showing me how to be a better researcher, and was always available to meet with me to discuss and map out future research plans for this project. I have learned a great deal in this lab. Dr. Smith also allowed me the room and flexibility to have a family here, and for that I am also very grateful. I would also like to thank Drs. David DeWitt and Michael Garavito for being on my committee, but more importantly for their help and support as well. I appreciate their time spent helping me with my research, as well as completing my degree.

I feel very lucky to have worked with such a large and supportive collaboration of people in this department. I thank all of the many Smith, DeWitt, and Garavito lab members, past and present, for all of their help and friendship, especially Beth Thuresson and Jill Rieke, as they were extremely helpful in showing me the ropes with these experiments, as well as good friends. I'd also like to thank Mike Malkowski for his help and good nature in supplying me with endless active site figures. Thank you also to Dr. Joe Leykam and the Macromolecular Structure Facility for their help with the HPLC experiments.

I'd like to thank my family and friends, including my parents, Paul, Nancy, Dave, Ted, Elaine, Sarah, Carol, Paul, and Madeleine for all their encouragement, support, and great laughs while I have been at Michigan State. Most importantly, I'd like to say thank you to Brian, not only for his killer commute these past few years, but for being a wonderfully supportive husband and friend, and to Megan and Baby Lakkides-to-be – quite possibly the two most important things I got out of grad school.

TABLE OF CONTENTS

LIST OF TABLES

LIST OF FIGURES

KEY TO ABBREVIATIONS

11-HETE	11-hydroxy-5*Z*,8*Z*,12*Z*,14*Z*-eicosatetraenoic acid
11-HpETE	11-hydroperoxy-5*Z*,8*Z*,12*Z*,14*Z*-eicosatetraenoic acid
12-HOTrE	12-hydroxy-9*Z*,13*E/Z*,15*Z*-octadecatrienoic acid
15-HETE	15-hydroxy-5*Z*,8*Z*,11*Z*,13*Z*-eicosatetraenoic acid
15-HpETE	15-hydroperoxy-5*Z*,8*Z*,11*Z*,13*Z*-eicosatetraenoic acid
18:2 *n*-6	linoleic acid
18:3 *n*-3	α-linolenic acid
20:5 *n*-3	eicosapentaenoic acid
20:3 *n*-6	eicosatrienoic acid
20:4 *n*-6	arachidonic acid (AA)
20:2 *n*-3	eicosadienoic acid
$cPLA_2$ / $sPLA_2$	cytosolic/secretory phospholipase A_2
DMEM	Dulbecco's modified Eagle medium
HHTrE (or HHT)	17-hydroxy-(5*Z*, 8*Z*,10*E*)-heptadecatrienoic acid
K_m	Michaelis-Menton constant
NSAID	non-steroidal anti-inflammatory drug
oPGHS-1	ovine prostaglandin endoperoxide H synthase -1
PBS	phosphate buffered saline
PGG_2	prostaglandin G_2
PGH_2	prostaglandin H_2
PGHS-1 / -2	prostaglandin endoperoxide H synthase -1 or -2
RP-HPLC	reverse-phase high pressure liquid chromatography
SDS-PAGE	sodium dodecyl sulfate - polyacrylamide gel electrophoresis
TBS	tris-buffered saline
TLC	thin-layer chromatography
TMPD	3,3,3',3'-tetramethylenephenylenediamine
V_{max}	maximum velocity of reaction

CHAPTER 1

LITERATURE REVIEW

Introduction

Prostaglandin endoperoxide H synthase (PGHS) catalyzes the first step of prostanoid biosynthesis. PGHS converts arachidonic acid to PGH_2, which is subsequently released from the enzyme to be converted to various prostaglandins or thromboxane A_2 by the appropriate synthases (1). The prostanoids, which include prostaglandins, prostacyclins, and thromboxanes, are involved in a large number of physiological responses, including vasodilation, platelet aggregation, renal function, gastric function, parturition, and ovulation, as well as various inflammatory responses. (2, 3).

The conversion by PGHS of arachidonic acid to PGH_2 is catalyzed in two separate reactions: a cyclooxygenase reaction, which converts arachidonic acid to PGG_2, and a peroxidase reaction, which converts PGG_2 to PGH_2 by a two-electron reduction. These two reactions are carried out in two separate active sites of the enzyme. The cyclooxygenase active site of PGHS is the pharmacological target of non-steroidal anti-inflammatory drugs (NSAIDs), which include aspirin, indomethacin, ibuprofen, and flurbiprofen, and also novel drugs which include celecoxib and rofecoxib (4, 5, 6). NSAIDs have been shown to inhibit platelet aggregation, inflammation, fever, and pain, and have effects on Alzheimer's disease and colon cancer (2) The mechanisms of PGHS activity and inhibition are the focus of a large body of research.

Prostanoid Biosynthesis

Arachidonic acid, a twenty carbon polyunsaturated fatty acid, is the precursor for eicosanoid formation, including the prostanoids (1, 7). Prostanoid formation is a three-step process which includes a) arachidonate release from membrane phospholipids, b) conversion of arachidonate to PGH_2 by PGHS, and c) conversion of PGH_2 to specific prostanoids, followed by their release from the cell. The overall process is shown in Figure 1.

Initially, arachidonic acid is cleaved from membrane phospholipids following hormonal activation of one of the phospholipase A_2s (PLA_2). Two classes of PLA_2 have been shown to be involved in the mobilization of arachidonic acid from phospholipids, cytoplasmic PLA_2 ($cPLA_2$) and several secretory PLA_2s ($sPLA_2$s) (8). $cPLA_2$ is an 85-kDa, Ca^{2+}-dependent isoform, requiring micromolar concentrations of intracellular Ca^{2+} for activity, while the $sPLA_2$s are 14-kDa isoforms that require millimolar concentrations of Ca^{2+} for activity. The $cPLA_2$ is believed to be the major mediator of agonist-induced arachidonic acid release in cells because of it's specificity in cleaving arachidonate groups from the *sn*-2 position of membrane phospholipids. Several $sPLA_2$s have also been shown to mobilize arachidonate, and subsequently increase prostanoid production, although specificity for arachidonate cleavage from phospholipids has not been shown as clearly as with $cPLA_2$ (9).Extracellular agents mobilize intracellular Ca^{2+} stores, which allows binding of Ca^{2+} to the Ca^{2+}-dependent lipid-binding (CaLB) domain of $cPLA_2$. Calcium binding of $cPLA_2$ is essential for translocation of the lipase to membrane phospholipids (10, 11). Activity of $cPLA_2$ is also potentiated by phosphorylation of Ser-505 (12). Release

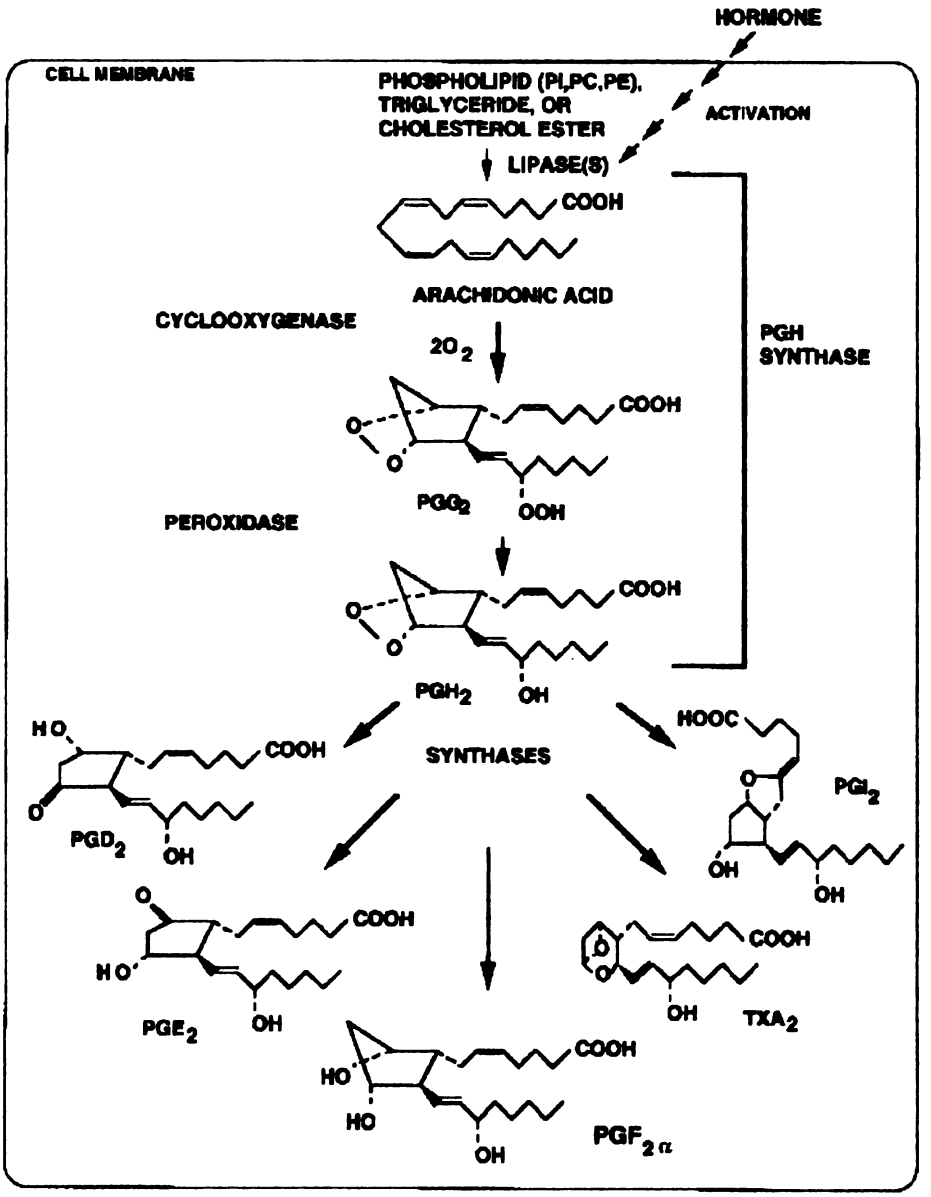

Figure 1. Structures and biosynthetic pathway for prostanoid synthesis.

of free arachidonic acid is increased upon activation of $cPLA_2$, which has a preference for phospholipids with arachidonate at the *sn*-2 position.

Free arachidonic acid next translocates to PGHS for the conversion to PGH_2. Upon entering the cyclooxygenase active site of PGHS, the *pro*-S hydrogen of C-13 is abstracted by a tyrosyl radical to yield an arachidonyl radical. This is followed by the addition of a molecule of oxygen to the C-11 position of the substrate, and the migration of the radical to this O_2 group. The oxygenated C-11 then cyclizes to the C-9 of arachidonate, resulting in the transfer of the radical back to the tyrosyl group. Another O_2 molecule is then added to the C-15 position, resulting in the endoperoxide intermediate PGG_2 (Figure 2). The peroxidase active site of PGHS then reduces the 15-hydroperoxyl group of PGG_2 to form PGH_2. Release of PGH_2 intracellularly allows for subsequent interaction with relevant synthases for conversion to prostanoid products. Cell specific expression of the different prostaglandin, prostacyclin, and thromboxane A_2 synthases dictate the final products formed. Prostanoids can then act in either an autocrine or paracrine fashion on cells via several specific G protein-linked prostanoid receptors on the plasma membrane. The activation of these receptors regulate the levels of various secondary messengers, such as cAMP, to mediate the large range of physiological responses described earlier (7).

PGHS-1 and PGHS-2

Two isoforms of PGHS have been identified, PGHS-1 and PGHS-2, which are encoded by two separate genes (13, 14). PGHS-1 was initially cloned and purified from ovine seminal vesicular gland tissue (15-18), and the murine (19), human (20), and rat (21) PGHS-1 cDNAs have since been cloned. Between

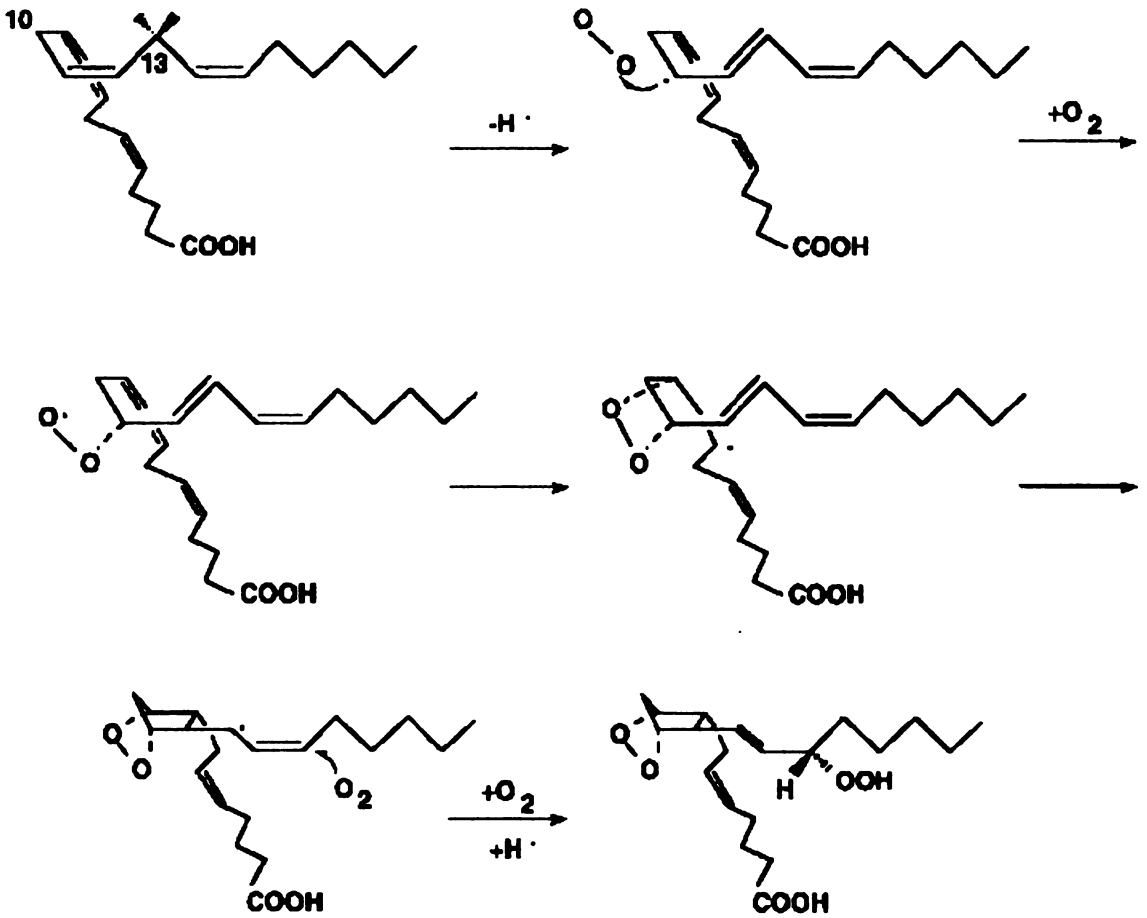

Figure 2. Model of mechanism of arachidonic acid conversion to PGG_2 by cyclooxygenase active site.

species, PGHS-1 shares a high (90%) amino acid identity. PGHS-1 mRNA and protein is constitutively expressed in most tissue types under normal physiological conditions, and is primarily involved in cellular housekeeping, maintaining the prostanoid biosynthesis necessary for tissue homeostasis. In 1991, PGHS-2 was discovered as an inducible form of the enzyme in cells stimulated with growth factors, mitogens, and phorbol esters (22-24). Unlike PGHS-1, this isoform is not detected in tissues under normal physiological conditions, with a sizable increase in expression seen upon stimulation of certain cell types. PGHS-2 cDNAs from mouse (23), chicken (24), rat (21), and human (22) have since been cloned.

Primary Structure

The primary structures of both isoforms share a 60% amino acid sequence identity within a species (Figure 3). The major differences in sequence between PGHS-1 and -2 are in the N-terminal and C-terminal regions of the isozymes. PGHS-1 has a sequence of hydrophobic residues within the signal peptide that are lacking completely in PGHS-2. Conversely, PGHS-2 contains a highly conserved (between species) 18-amino acid cassette at the C-terminus, whose function has not yet been determined.

The theoretical molecular mass of PGHS-1 and -2 is 66 kDa and 67 kDa respectively, with apparent molecular masses of 72 kDa for PGHS-1 and both 74 and 72 kDa for PGHS-2. The 72 kDa masses can be attributed to the addition of carbohydrate groups at three *N*-glycosylation sites in both PGHS-1 and -2 (Asn68, Asn144, Asn410). Glycosylation of all three sites is essential for enzyme activity in both isozymes (25). The 74 kDa mass of PGHS-2 is attributed to an

Figure 3. Comparison of amino acid sequences of various species of PGHS-1 and PGHS-2. Numbering of residues corresponds to murine PGHS-1 and begins with the Met translational start site.

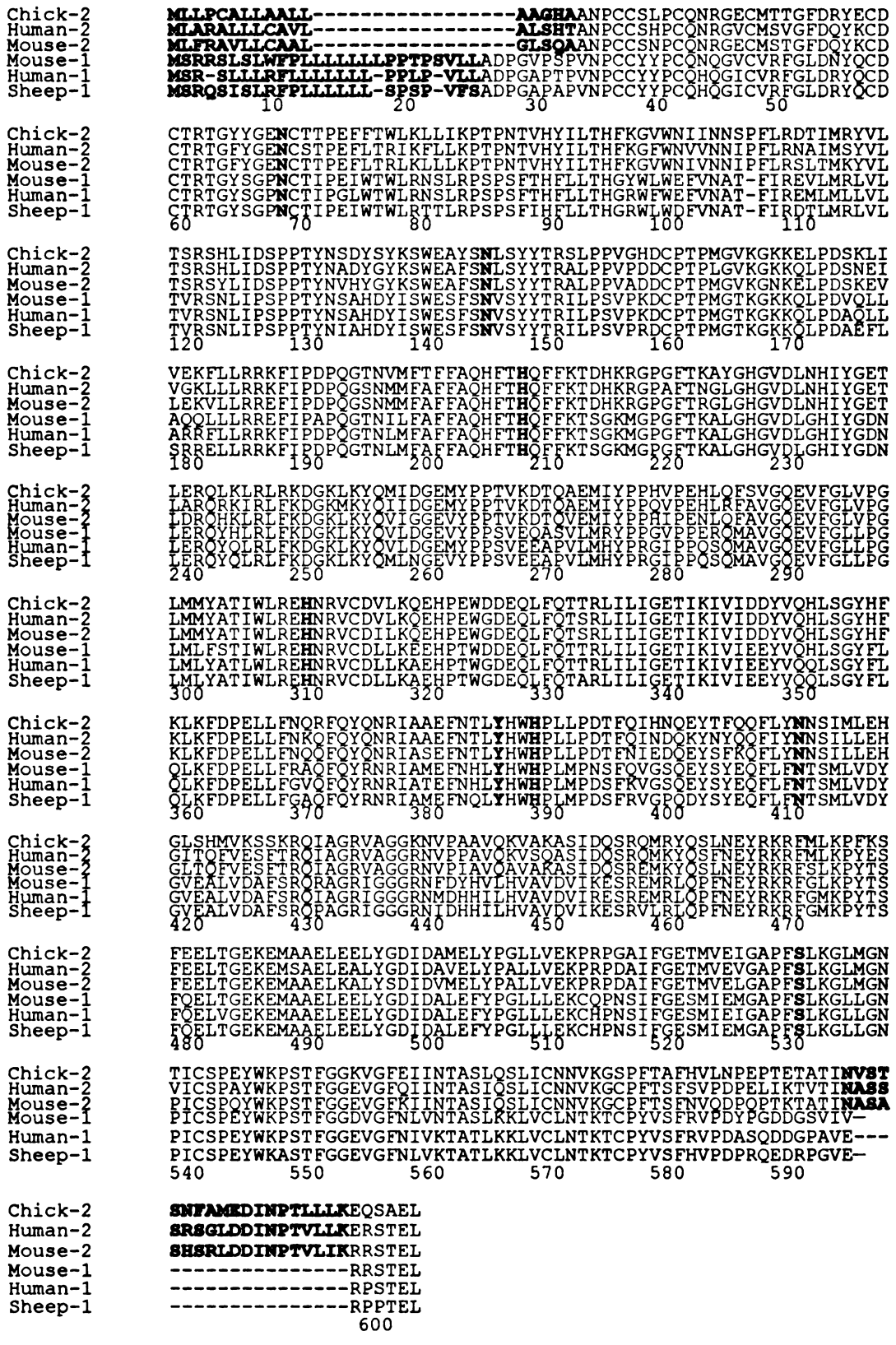
Chick-2
Human-2
Mouse-2
Mouse-1
Human-1
Sheep-1
10 20 30 40 50
60 70 80 90 100 110
120 130 140 150 160 170
180 190 200 210 220 230
240 250 260 270 280 290
300 310 320 330 340 350
360 370 380 390 400 410
420 430 440 450 460 470
480 490 500 510 520 530
540 550 560 570 580 590
600

Figure 3.

inefficient N-glycosylation at a unique fourth site, Asn580, whose glycosylation has no effect on the enzymatic activity of PGHS-2 (25). Otherwise, the enzymes share a remarkable similarity in sequence within a species, with an EGF domain, three *N*-glycosylation sites, and all catalytically important residues conserved in both PGHS-1 and PGHS-2.

Localization of PGHSs

PGHS-1 and -2 are both membrane-associated and localize to both the endoplasmic reticulum (ER) and the nuclear envelope (26, 27). Initially, immunofluorescence labeling showed a difference in intracellular localizations of the two isoforms (28). However, more recently, using immunogold labeling and electron microscopic methods, the localizations of PGHS-1 and PGHS-2 were found to be in similar proportions between the luminal ER membrane and the inner and outer nuclear envelope membranes (29).

Crystal Structures

In 1994, the crystal structure of ovine (o) PGHS-1 was first solved (30). The structure confirmed the presence of three folding units: an EGF homology domain, a membrane-binding domain, and a catalytic domain containing both cyclooxygenase and peroxidase catalytic sites (Figure 4). From solubilization and crystallization studies of PGHSs, it has been shown that the isozymes function as homodimers, forming an interface between the EGF homology domain of each monomer. Immunofluorescence and crystallization studies also show that there are similar membrane-binding domains for each isozyme, made up of four

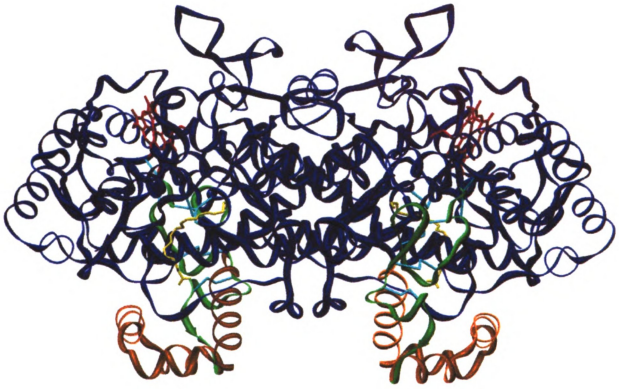

Figure 4. Crystal structure of oPGHS-1. The major folding units are shown in green (EGF domain), orange (membrane binding domain), and blue (catalytic domain). The structure is shown as a dimer, with arachidonic acid bound in the cyclooxygenase active site. (Images in this thesis are presented in color.)

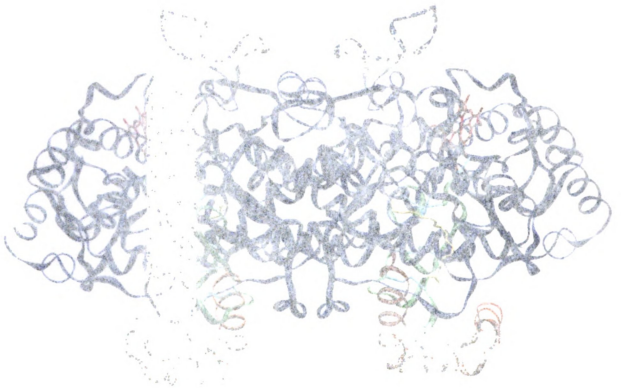

amphipathic α-helices, which are believed to interact with a single leaflet of the membrane bilayer (30, 31).

The crystal structure of PGHS-1 complexed with the NSAID flurbiprofen show the drug localized to a long, hydrophobic channel within the cyclooxygenase active site. The opening of this site begins with the membrane-binding domain, and extends into the PGHS catalytic domain, with one active site in each monomer. Presumably, the arachidonic acid substrate would be cleaved from the membrane lipids and could directly access the hydrophobic cyclooxygenase active site channel. From the available crystalized enzyme-inhibitor complexes, and from what was believed to be the cyclooxygenase mechanism, it was possible to build a preliminary model of the arachidonate substrate in the cyclooxygenase active site. The peroxidase active site was found to be a shallow channel containing a heme group that is accessible to PGG_2 substrate. In 1996, the crystal structure of human PGHS-2 was determined, complexed with two different inhibitors, and found to have a tertiary and quaternary structure very similar to that of PGHS-1 (32, 33). One important difference between the two cyclooxygenase active sites was the substitution of Ile-523 in PGHS-1 with a Val in PGHS-2, contributing to a larger overall volume in PGHS-2 than PGHS-1.

Very recently, the crystal structure of Co^{+3}-heme ovine PGHS-1 complexed with arachidonic acid was solved (34). This structure was able to show specific substrate-enzyme interactions within the cyclooxygenase active site (Figure 5). While the original PGHS-1 crystal structure confirmed the position of relevant active site residues near the "top" of the hydrophobic channel, such as Tyr-385, this later model showed conclusively that the arachidonate substrate

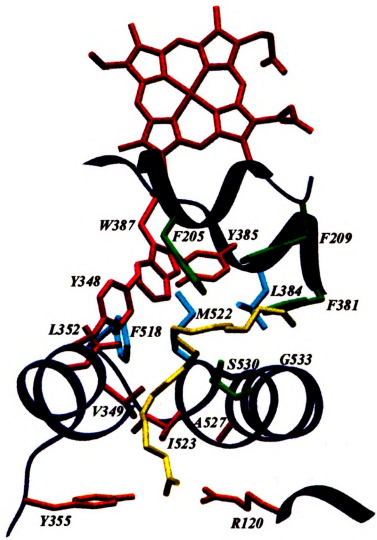

Figure 5. Active site of crystal structure of Co^{+3}-heme oPGHS-1 complexed with arachidonic acid. Critical and important residues noted in the text are labeled accordingly. (Images in this thesis are presented in color.)

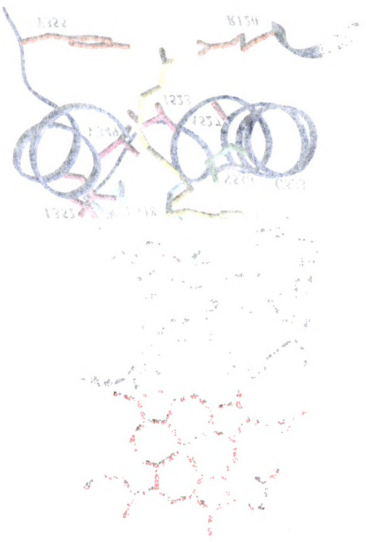

(from C-13 to C-20) extends past Tyr385 into the catalytic domain of the enzyme, in a continuation of the active site channel.

Active Sites of PGHSs

Residues critical to PGHS activity were initially identified via site-directed mutagenesis and EPR studies. In 1988, Ruf and co-workers used EPR to detect the generation of a tyrosyl radical with the interaction of PGHS and arachidonic acid (35), and therefore involved in the initial, rate-limiting step of the cyclooxygenase reaction. The relevant residue was later identified as Tyr385, shown to be critical for the enzymatic activity of PGHS (36). Both PGHS-1 and -2 have one iron (Fe III) protoporphyrin IX group per subunit that binds a heme group (15, 37, 38), and is essential for both cyclooxygenase and peroxidase activities (37). This heme is coordinated by histidine residues, and site-directed mutagenesis studies were able to find those His residues essential for enzymatic function (39, 40). His207 was found to act as the distal heme ligand, and His-388 as the proximal heme ligand. His388 is required for both cyclooxygenase and peroxidase activities. Another histidine residue, His386, was found to be required for peroxidase, but not cyclooxygenase activity (39). The proximity of these neighboring residues to both the cyclooxygenase and peroxidase active sites, combined with the Tyr385 residue being essential for cyclooxygenase activity, supported a model in which the active sites were separate yet near one another in the catalytic domain. This model was verified by the crystallographic data (30).

Serine 530, while not shown to be a catalytically critical residue, is the active site residue that is acetylated by aspirin to inhibit cyclooxygenase activity

(19, 41, 42). The crystallographic studies of PGHS identified Arg120 as a residue located at the mouth of the cyclooxygenase active site channel (30). The presence of this polar residue in an otherwise hydrophobic environment, and it's proximity to the carboxyl group of flurbiprofen when in the active site, suggested that this residue interacted with the carboxyl group of arachidonic acid. Site-directed mutagenesis indicated that Arg120 is essential for substrate binding, suicide inactivation, and inhibitor binding in oPGHS-1 (43, 44). However, in PGHS-2 the comparable residue (Arg106) was shown to be much less important for binding of the substrate to the active site (45).

As mentioned earlier, the only residue in the cyclooxygenase active site not identical between PGHS-1 and PGHS-2 is Ile523, which is a smaller valine residue in PGHS-2 (Val509). The crystal structures of both isozymes found that the PGHS-2 active site volume to be 17% larger than that of PGHS-1 (32). This one residue difference has also been shown to affect NSAID binding in the two isozymes (46, 47), with the Val509 of PGHS-2 shown in itself to confer selectivity of PGHS-2-selective inhibitors (46). Conversely, a double mutant of PGHS-1 (His513 → Arg and Ile523 → Val) was able to convert PGHS-1 into an enzyme sensitive to PGHS-2-selective inhibitors (48).

Substrate Specificity of PGHS

Although the structural properties of PGHS-1 and PGHS-2 show little difference between isoforms, there is considerable biochemical evidence that the two enzymes bind substrates differently. Both PGHS-1 and PGHS-2 show a preference for arachidonate (20:4 *n*-6) as substrate, with comparable V_{max}s and

similar K_ms (~ 5 μM) (49, 50). Various other 20-carbon and 18-carbon polyunsaturated fatty acid derivatives can compete with arachidonate for oxygenation by PGHS. These include dihomo-γ-linolenic acid (20:3 *n*-6) (51), eicosapentaenoic acid (20:5 *n*-3) (52), linoleic acid (18:2 *n*-6) (53), and α-linolenic acid (18:3 *n*-3)(49). These substrates are all converted to various classes of prostanoids by PGHS, but the specificity of some of these substrates between the two isoforms has been shown to differ. The 20-carbon substrates 20:4 and 20:3 were better substrates with PGHS-1 and PGHS-2 than 20:5 and the 18-carbon substrates 18:2 and 18:3. Yet overall PGHS-2 was better able to utilize the poorer 18-carbon substrates than PGHS-1 under experimental conditions (49). As mentioned earlier, PGHS-2 also lacks the apparent need for the Arg106 residue in order to "anchor" substrate (via an ionic bond to the carboxylate group of the substrate) into the cyclooxygenase active site (45).

Substrate utilization of the PGHSs has also been examined in inhibitor studies, specifically with the acetylation of the relevant serine residue (Ser530 in PGHS-1 and Ser516 in PGHS-2) by aspirin. (41, 50, 54). While aspirin completely inhibited arachidonate metabolism in PGHS-1, aspirin-acetylated PGHS-2 was able to metabolize arachidonate with a monohydroxy addition to form 15*R*-hydroxyeicosatetraenoic acid (15*R*-HETE) (55). Mutational studies of the Ser530/516 helped confirm that this difference in arachidonic acid utilization could be attributed to an overall larger active site in PGHS-2 (54, 56).

Purpose of Research

This thesis focuses on research into the functional roles of several additional residues shown to make up the hydrophobic active site channel oPGHS-1. The first set of residues are those near the critical Tyr385 residue, and include Trp387, Met522, Phe518, and Leu384. The fifth residue investigated is Gly533, located in the highly conserved region surrounding Ser-530, the site of aspirin acetylation.

The goal of these studies was to determine if these selected residues are involved in any step of PGG_2 formation, and to characterize their roles in maintaining the enzymatic integrity of oPGHS-1 with arachidonic acid substrate. In the cases where the mutant enzyme was still functional, in that it was still able to utilize molecular oxygen, the subsequent products formed by the mutant enzyme were identified and quantified for comparisons to the native enzyme counterparts. The effect of some of these mutations on the oxygenation of other fatty acid substrates was also investigated. These studies contribute to number of other active site residues being studied in our laboratory, and were performed in the hopes of better defining and understanding the PGHS-1 and PGHS-2 active sites.

CHAPTER 2

STUDIES TO DETERMINE THE ROLES OF TRP387, MET522, PHE518, AND LEU384 oPGHS-1 IN CYCLOOXYGENASE ACTIVITY, PRODUCT FORMATION, AND SUBSTRATE INTERACTION

Introduction

Examination of the original oPGHS-1 crystal structure, as well as previous cyclooxygenase active site mutational studies, suggested several residues that could be involved in the cyclooxygenase process of oPGHS-1. The selected residues for these studies, Trp387, Met522, Phe518, and Leu384, are all located in the area of the active site where there is an L-shaped bend in the hydrophobic channel, and all are along the outer edge of this channel (Figures 6 and 7). These residues are conserved in all species of PGHS-1 and PGHS-2 (Figure 3 of literature review). The location of these residues indicated possible roles in enzyme catalysis or in maintaining the conformation and positioning of arachidonic acid (or other fatty acid substrates) during the endoperoxide ring formation of PGG_2 between C-9 and C-11. Trp387 was also of initial interest due to it's proximity to residues Tyr385, His386, and His388, all of which are critical to either cyclooxygenase or peroxidase activities, or both (36, 39, 41). The Trp387 mutants studied here were all previously made in this laboratory by Linda Hsi and Elizabeth Thuresson, and cyclooxygenase and peroxidase activities of some of these mutants have already been reported (57).

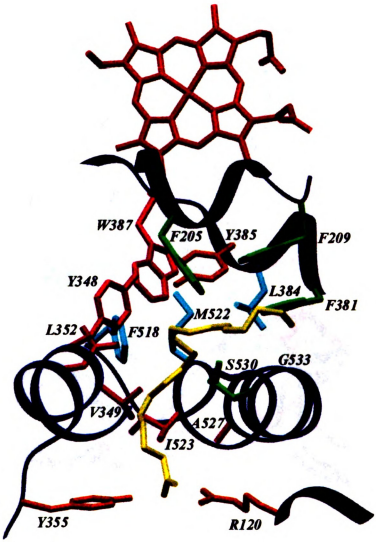

Figure 6. Crystal structure of cyclooxygenase active site of Co^{+3}-heme oPGHS-1 complexed with arachidonic acid (front view). Residues mutated are shown with native side chains, and include the following: Trp387 (pink), Met522, Phe518, Leu384 (all light blue), Gly533 (location shown on α-helix, dark blue), and Ile523 (also pink). Critical residues Tyr385 and Arg120 are shown in orange. Arachidonic acid is shown in yellow. (Images in this thesis are presented in color.)

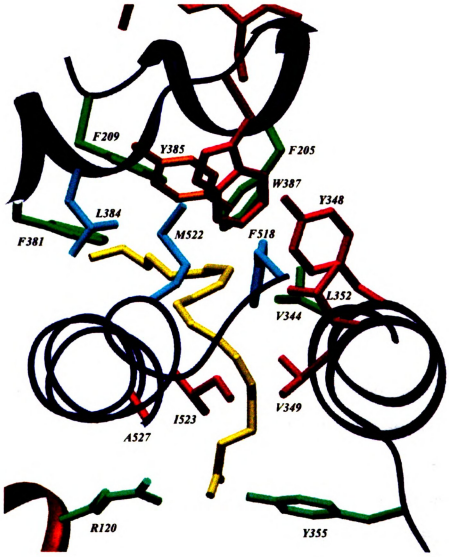

Figure 7. Crystal structure of cyclooxygenase active site of Co^{+3}-heme oPGHS-1 complexed with arachidonic acid (back view). Same residues and colors as shown in Figure 6. (Images in this thesis are presented in color.)

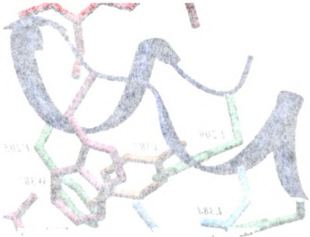

More recently, the crystal structure of Co^{+3}-heme oPGHS-1 complexed with arachidonic acid in the cyclooxygenase active site allowed for a more accurate analysis of which of these active site residues actually contacts the substrate. Consequently, it was shown that the benzene ring of the indole group of Trp387 is positioned within 4 Å of the C-11 and C-12 of bound arachidonic acid, the minimal distance for a van der Waals interaction (Table 1). The other residues examined, Leu384, Met522 and Phe518, although involved in making up the hydrophobic active site channel, were found to be less likely to contact arachidonic acid, with distances of 4-6 Å from bound substrate (58). However, when these studies were performed, the exact positioning of arachidonic acid to these residues was not yet known.

The mutated residues examined here were initially investigated for their role in overall catalysis, to see if any were critical to enzyme function. Furthermore, they were studied to determine which products these mutants made, and in what proportions, as compared to the native enzyme. The major role of the native enzyme is the production of PGG_2-derived products, including HHTre (17-hydroxy-(5*Z*, 8*Z*, 10*E*)-heptadecatrienoic acid), PGD_2, PGE_2, and $PGF_{2\alpha}$. But PGHSs also have some lipoxygenase activity, which produces small amounts of monohydroxy products 11-hydroperoxy-5*Z*,8*Z*,12*E*,14*Z*-eicosatetraenoic acid (11-HpETE) and 15-hydroperoxy-5*Z*,8*Z*,11*Z*,13*E*-eicosatetraenoic acid (15-HpETE), which are further reduced to 11-HETE and 15-HETE (60, 61). In some cases, the stereochemistry of some of these products from mutant oPGHS-1 was also determined for comparison to the native enzyme.

Table 1. Contact distances between Co^{+3}-heme oPGHS-1 and bound arachidonic acid and other active site residues. Only those distances of 4 Å or less are deemed likely to be making van der Waal contacts. Other distances, between 4 - 6 Å are also included as reference.

Residue	Atom	Residue	Atom	Distance (Å)
Trp387	CZ2	20:4	C-11	3.95
	CH2	20:4	C-11	3.38
	CH2	20:4	C-12	3.65
Ile523	CG2	20:4	C-2	3.80
	CG2	20:4	C-5	3.31
	CG2	20:4	C-6	3.44
Gly533	CA	20:4	C-20	3.63
Leu384	CD1	20:4	C-9	5.98
	CD2	20:4	C-9	4.92
	CD2	Trp 387	NE1	4.28
	CD2	Trp 387	CE2	4.79
	CD2	Tyr 385	CG	4.68
Met 522	CG	20:4	C-8	5.22
	CE	Trp 387	NE1	4.33
	CE	Trp 387	CD1	3.72
	SD	Trp 387	NE1	3.60
Phe 518	CZ	20:4	C-6	4.39
	CZ	20:4	C-8	4.84
	CE2	20:4	C-6	4.50
	CE1	Trp 387	CZ2	4.17

Finally, the ability of some of these mutated enzymes to utilize fatty acid substrates other than arachidonic acid was investigated.

Materials and Methods

Materials - Dulbecco's modified Eagle's Medium (DMEM) was purchased from Gibco. Calf serum and fetal bovine serum were from HyClone. Arachidonic acid, linoleic acid, eicosapentaenoic acid, dihomo-γ-linolenic acid, and α-linolenic acid, as well as all TLC and HPLC standards were purchased from Cayman Chemical Co., Inc. [1-^{14}C]-Arachidonic (50-55 mCi/mmol) was from Dupont NEN Life Science Products. Primary antibodies used for Western blotting were raised in rabbits against purified oPGHS-1 and purified as an IgG fraction (27). Goat anti-rabbit IgG horseradish peroxidase conjugate was from BioRad. Oligonucleotides used as primers for mutagenesis and sequencing were prepared by the Michigan State University Macromolecular Structure and Sequencing Facility. Other reagents were purchased from common commercial sources.

Preparation of mutants by site directed mutagenesis - The Trp387 mutants were previously prepared in our laboratory (57). The Met522 and Phe518 mutants of oPGHS-1 were prepared using a BioRad Muta-Gene kit, as previously described (59), starting with M13mp19-ovine PGHS-1, which contains a 2.3-kilobase *SalI* fragment encoding native oPGHS-1. The oligonucleotides used for mutagenesis are shown in Table 2. Phage samples were sequenced using the dideoxy method of Sequenase (ver. 2.0, U.S. Biochemical Corp.). The replicative forms of the mutant M13mp19-oPGHS-1s were prepared from phage cultures, digested with *SalI*, and the resulting 2.3-kilobase oPGHS-1 cDNA

Table 2. Oligonucleotide primers used for preparing oPGHS-1 mutants. Mutants were prepared using two different procedures. Trp387, Met522, and Phe518 mutants were made using the BioRad Mutagene kit (see Materials and Methods), and short, single-stranded oligonucleotide primers were constructed. The Leu384, Gly533, and Ile523 mutants were made using the Strategene QuikChange system, and longer, double-stranded primers were constructed (only the + strand sequence is shown). Mutation sites are underlined, including (in some cases) silent mutations that were designed for verification of the mutant. The numbering is based on cDNA of oPGHS-1 (18).

Mutation	Oligonucleotide primer
W387A	5'-^{1247}AGCTGTACCACGCGCACCCGCTC^{1269}-3'
W387F	5'-^{1247}AGCTGTACCACTTCCACCCGCTCAT^{1271}-3'
W387L	5'-^{1247}AGCTGTACCACCTGCACCCGCTC^{1269}-3'
W387R	5'-^{1247}AGCTGTACCACAGGCACCCGCTCAT^{1271}-3'
W387S	5'-^{1247}AGCTGTACCACTCGCACCCGCTCAT^{1271}-3'
M522A	5'-^{1650}CTTTGGGGAGAGTGCGATAGAAATGGG^{1676}-3'
M522L	5'-^{1650}CTTTGGGGAGAGTCTGATAGAAATGGG^{1676}-3'
M522I	5'-^{1650}CTTTGGGGAGAGTATCATAGAAATGGG^{1676}-3'
F518A	5'-^{1640}CGAACTCCATCGCTGGGGAGAGTAT^{1664}-3'
F518L	5'-^{1640}CGAACTCCATCTTGGGGGAGAGTAT^{1664}-3'
F518M	5'-^{1640}CGAACTCCATCATGGGGGAGAGTAT^{1664}-3'
F518Y	5'-^{1640}CGAACTCCATCTATGGGGAGAGTAT^{1664}-3'
L384A	5'-^{1219}CGCAACCGCATCGCCATGGAATTCAA CCAGGCCTACCACTGGCACCCG^{1266}-3'
L384F	5'-^{1219}CGCAACCGCATCGCCATGGAATTCAA CCAGTTCTACCACTGGCACCCG^{1266}-3'
L384V	5'-^{1219}CGCAACCGCATCGCCATGGAATTCAA CCAGGTGTACCACTGGCACCCG^{1266}-3'
G533A	5'-^{1681}CCTTTTTCCCTTAAGGCTCTCTTAGG AAACCCCATC^{1716}-3'
I523V	5'-^{1645}CCATCTTTGGGGAGTCCATGGTAG AAATGGGGGCTC^{1681}-3'

fragments were purified and subcloned into pSVT7. The orientation of each mutant insert was verified with digestion with *PstI*. Plasmids were purified by CsCl density gradient ultracentrifugation. The mutations were reconfirmed by sequencing of the pSVT7 constructs. The Leu384 mutants were prepared using a QuikChange site-directed mutagenesis kit (Stratagene, LaJolla, CA), with the pSVT7 oPGHS-1 plasmid as a template in polymerase chain reactions (PCR) for constructing the mutant forward and reverse primers, seen also in Table 2. The PCR cycling parameters were 16 cycles of 95 °C for 30 s, 55 °C for 1 min, 68 °C for 2 min. Purification and subcloning of plasmids were essentially the same as described above.

Transfection of COS-1 cells with recombinant oPGHS-1 - COS-1 cells (ATTC CRL-1650) were grown in DMEM containing 2% fetal bovine serum and 8% calf serum, in a water-saturated 7% CO_2 atmosphere until near confluency. Cells were transfected with a pSVT7 plasmid containing cDNA coding native or mutant oPGHS-1, using a DEAE-dextran/chloroquine method previously reported (19, 27). Sham-transfected cells were also prepared in a similar manner. Forty hours post-transfection the cells were harvested by scraping in ice-cold phosphate-buffered saline (PBS), centrifuged for 1200 rpm for 5 min, and resuspended in 0.1 M Tris-HCl, pH 7.5.

Preparation of microsomes - Cells pelleted from 25-40 plates were resuspended in 5 mL of ice-cold 0.1 M Tris-HCl, pH 7.4, and disrupted by sonication. The

sonicated cells were centrifuged at 10,000 rpm for 10 min at 4 °C. The resulting supernatants were ultracentrifuged at 45,000 rpm for 50 min at 4 °C using a Beckman SW50.1 swinging rotor. Microsomal membrane pellets were resuspended by homogenization in 20-30 µL of 0.1 M Tris-HCl, 1 mM phenol per culture dish. Protein concentrations were measured at 595 nm using Bio-Rad Bradford protein assay reagent.

Cyclooxygenase assays - Cyclooxygenase assays were performed by measuring the initial rate of O_2 consumption at 37 °C, using a Yellow Springs Instruments Model 5300 oxygen electrode. A standard assay mixture contained 3 mL of 0.1 M Tris-HCl, 1 mM phenol, pH 8.0, 85 µg bovine hemoglobin (as heme source), and 100 µM arachidonic acid. Reactions were initiated by the addition of microsomal protein (approximately 100-200 µg), in a volume of 20-80 µL, to the assay mixture, and initial rates of oxygen uptake were determined. Preincubation of 200 µM flurbiprofen inhibitor to the assay mixture determined that the oxygen consumption was due to cyclooxygenase activity. For studies of substrate specificity, 100 µM concentrations of 20:3 *n*-6, 18:2 *n*-6, 20:5 *n*-3, 20:2 *n*-6, and 18:3 *n*-3 were used. Determinations of K_m were performed using decreasing concentrations of arachidonic acid, and again measuring the initial oxygen uptake.

Peroxidase assays - Peroxidase assays were performed spectrophotometrically on a Perkin-Elmer model 552A Double Beam UV-visible spectrophotometer by

measuring the oxidation of 3,3,3',3'-tetramethylenephenylenediamine (TMPD) at 611 nm over time. A standard assay mixture contained 0.1 mM TMPD, 1.7 μM hematin, approximately 100 μg protein, and 0.1 M Tris-HCl, pH 8.0 to a total volume of 3 mL, and reactions were initiated by the addition of 100 μL of 0.3 mM H_2O_2.

Western blotting - Protein samples were separated on 10% polyacrylamide gels containing 0.1% SDS (SDS-PAGE) and then transferred to 0.45 μm nitrocellulose membranes using a Bio-Rad Trans-blot unit and transfer buffer containing 25 mM Tris, 192 mM glycine, and 20% methanol. Membranes were blocked for non-specific protein absorption with incubation for at least 20 min in Tris-buffered saline (20 mM Tris-Cl, 137 mM NaCl, pH 7.6) containing 0.1% Tween-20 detergent (TBS-T) and 3% non-fat dry milk. The membranes were then incubated for 2 h at 25 °C in a 1:1000 dilution of an affinity purified isozyme-specific rabbit antisera for oPGHS-1 (Gloria), followed by 3 X 10 min washes in TBS-T/1% milk. The membranes were then incubated for 1 h at 25 °C in a 1:2500 dilution of horseradish peroxidase-conjugated goat anti-rabbit IgG antibody (BioRad), followed by 2 X 10 min washes in TBS-T/1% milk, and one 10 min wash in TBS-T alone. The proteins were visualized by chemiluminescence using Amersham ECL reagents and exposure to Kodak XAR film.

Characterization of arachidonate derived products by thin layer chromatography - Cell suspensions from transfected cells were disrupted by sonication and were

measured at 595 nm for protein concentration using Bio-Rad Bradford protein assay reagent. Aliquots of 100 µg of protein were incubated for 30 min at 37 °C with 6.8 µg bovine hemoglobin and various concentrations (20-100 µM) of [1-^{14}C]-arachidonic acid. Reactions were stopped by the addition of 1.4 mL chloroform: MeOH (1:1, v/v), and then centrifuged for 10 min at 3000 rpm to remove cellular debris. Supernatants were transferred to clean tubes, and 0.6 mL chloroform and 0.32 mL 0.88% formic acid was added. The organic layer was separated by centrifugation at 3000 rpm for 5 min, extracted out into new tubes, and dried under N_2. The samples were resuspended in 50 µL chloroform and spotted onto Silica Gel 60 thin layer chromatography plates. The plates were developed twice in benzene: dioxane: acetic acid: formic acid (82:14:1:1, v/v/v/v). The products were visualized either by autoradiography using a Molecular Dynamics Storm 820 phosphorimager and ImageQuant software, or by exposure to Kodak XAR film, followed by scraping of product bands and liquid scintillation counting. Radioactive bands were identified by comparison with the authentic standards. Actual product values were calculated by subtracting out the corresponding values of sham-transfected samples.

Reverse-phase HPLC - Native and mutant microsomal preparations of transfected COS-1 cells and semi-purified side-fractions of oPGHS-1 were incubated with 100 µM arachidonic acid for 1 min at 37 °C, and extracted as the reactions described above. The products were dried down with N_2 gas and resuspended in a 1:1 (v/v) mixture of H_2O with 0.1% glacial acetic acid and

acetonitrile with 0.1% glacial acetic acid. The 15-HETEs and 11-HETEs were separated by reverse phase (RP)-HPLC using a C-18 Vydac column (Hesperia, CA) and were detected with a Waters model 600 HPLC and a 990 photo diode array detector monitoring at an absorbence of 234 nm. The H_2O/0.1% acetic acid was the polar mobile phase and the acetonitrile/0.1% acetic acid was the eluting phase. The elution of the HETE products was performed at a rate of 1 mL/min, and followed this profile: 0-30 min, 30% acetonitrile; 30-100 min, 50% acetonitrile; 100-125 min, 75% acetonitrile; 125-130 min, 100% acetonitrile. The retention times were 36 min for 15-HETE, and 38 min for 11-HETE, and were verified by coinjection with authentic standards.

Chiral HPLC of Methylated 11-HETE and 15-HETE - The collected fractions of 11-HETE and 15-HETE were converted to their methyl esters by reaction with diazomethane, prepared from Diazald (*N*-methyl-*N*-nitroso-*p*-toluenesulfonamide) (Aldrich). The methyl esters were analyzed by chiral-phase HPLC on a Chiralcel OC column (Daicel Chemical Industries, Osaka, Japan) eluted at a rate of 0.5 mL/min with hexane/2-propanol (98:2, v/v). The retention times were 25 min and 27 min for 15*R*- and 15*S*-HETE respectively, and 26 min and 28 min for 11*R*-HETE and 11*S*-HETE respectively, and were verified by coinjection with authentic racemic standards.

Results

Native oPGHS-1 and all mutants were transiently expressed in COS-1 cells and microsomal membrane fractions of each were assayed for initial cyclooxygenase activity (V_{max}), using 100 μM arachidonic acid as substrate, and peroxidase activity, using H_2O_2 and TMPD as co-substrates. The individual products of some of the cyclooxygenase-active of these mutants were separated by thin-layer chromatography and quantified by densitometry. In all cases, sham-transfected cells were analyzed for activity alongside cells transfected with native oPGHS-1 or the various oPGHS-1 mutants. The results are summarized in Table 3, and the data shown are normalized to the relative activities of the native enzyme.

Trp387 - The previous studies of W387F, W387R, and W387S had shown that W387R and W387S lack cyclooxygenase activity, with W387R also lacking any peroxidase activity, and W387S retaining 4% of the peroxidase activity of the native enzyme (57). However, W387F maintained 38% of native cyclooxygenase activity and 53% of the native peroxidase activity (57). More recent experiments confirmed these findings, with nearly identical results (W387F having 44% native cyclooxygenase activity and 57% native peroxidase activity, see Table 3). Two other hydrophobic mutants were prepared, W387A and W387L, and initial cyclooxygenase and peroxidase activities were measured. W387A lacked cyclooxygenase activity, but still had 60% of the native peroxidase activity. W387L had a low rate of cyclooxygenase activity, at 7% of native, yet retained at

Table 3. Kinetic properties and product analyses for oPGHS-1 cyclooxygenase active site mutants with arachidonic acid substrate. V_{MAX} determinations and product analyses were determined at high concentrations (35-100 μM) of arachidonic acid. Peroxidase activity was measured spectrophotometrically as described in the text. All values are corrected to consider that 2 moles of O_2 are consumed for each mole of arachidonic acid for dihydroxy products, and 1 mole of O_2 was consumed for each mole of arachidonic acid for monohydroxy products.

ENZYME	CYCLOOXYGENASE (with 20:4)			PEROXIDASE (% native)	11-HETE (% of total products)	15-HETE (% of total products)
	V_{MAX} (% native)	K_m (μM)	V_{MAX}/K_m			
Native oPGHS-1	100	2	50	100	2.5 (11*R*)	2.5 (15*R/S*)
Sham	0	--	--	0	--	--
W387A	0	--	--	60	--	--
W387L	7	8	0.88	123	39.2	1.6
W387F	44	25	1.8	57	35.8	1.3
W387R	0	--	--	0	--	--
W387S	0	--	--	4	--	--
F518A	38	20	1.9	23	8.8	2.2
F518L	99	4.8	21	130	4.2	3.5
F518M	70	--	--	55	5	4.5
F518Y	44	4	11	30	4.2	9.3
M522A	65	2.3	28	48	3.8	3.3
M522L	46	3.4	14	28	2.5	0
M522I	69	--	--	105	3.1	2.9
L384A	29	--	--	61	2.8	3.8
L384F	8.3	--	--	90	--	--
L384V	23	--	--	23	1.5	0.8

least native peroxidase activity (reported at 123% of native). Western transfer blotting of all the Trp387 mutants indicated that these mutants express in COS-1 cells at relatively the same level as the native enzyme (Figure 8A). The K_ms of the two Trp387 mutants that retained some cyclooxygenase activity were measured with arachidonic acid, with W387F having a 10-fold increase in K_m (25 μM) from that of native enzyme (about 2 μM) and W387L having a K_m of 8 μM.

The products formed by W387F and W387L were determined by using excess of arachidonic acid incubated with the enzyme, and separating by thin-layer chromatography. Figure 9 shows the separation of the major radioactive products, and results in Table 3 are expressed as the percent of total converted product from arachidonic acid. Both mutants formed the same products from arachidonic acid as native oPGHS-1, including the PGG_2-derived products (HHTre, PGD_2, PGE_2, and $PGF_{2\alpha}$), and the monohydroxy products 11-HETE and 15-HETE. In the native enzyme preparations, 95% of the products were derived from PPG_2, and on average the 11-HETE and 15-HETE were expressed at 3% and 2%, respectively. However, W387F and W387L were both found to form large amounts of 11-HETE, which contributed to 36% of the total products for W387F, and 39% of the total products for W387L. In both cases, the PGG_2-derived products made up most of the remainder of the total products, with the 15-HETE production slightly lower than native for both mutants.

Thin-layer chromatography is not adequate to characterize the chiral isoforms of the monohydroxyl products of the native and mutant enzymes. Extracts from native oPGHS-1 and W387F were incubated with arachidonic acid

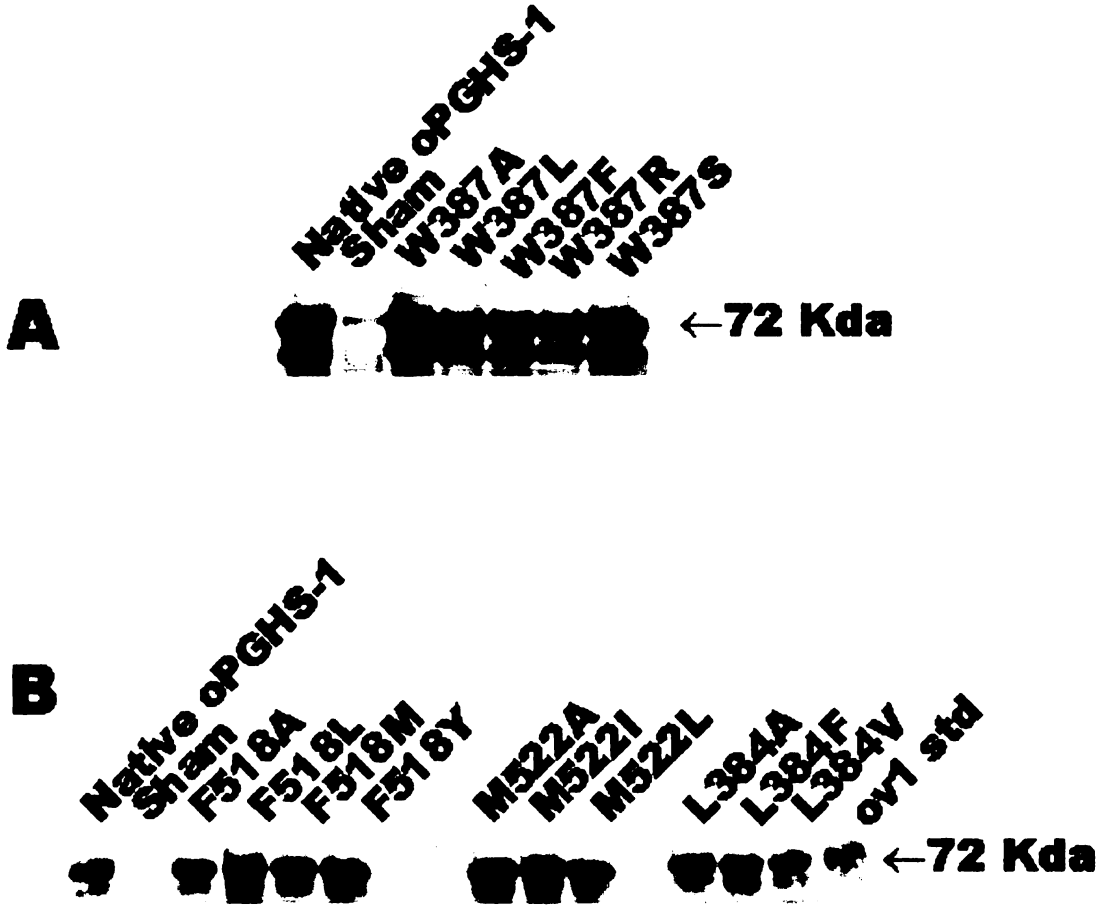

Figure 8. Western blot analysis of native and mutant oPGHS-1s. A) Trp387 oPGHS-1 mutants, and B) Phe518, Met522, and Leu384 oPGHS-1 mutants. Native oPGHS-1 and sham-transfected samples were run concurrently. From equal amounts of native and mutant oPGHS-1 total protein expressed in COS-1 cells, as described in the text.

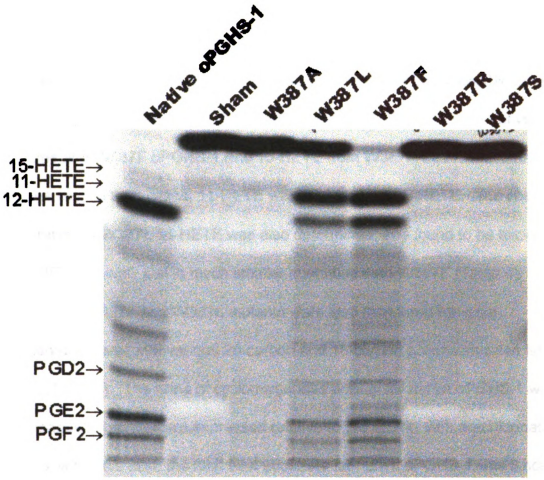

Figure 9. Thin-layer chromatograms of products formed from [1-^{14}C] arachidonic acid by native oPGHS-1 and Trp387 mutants. Broken cell preparations (1 mg of protein) of COS-1 cells transfected with native or mutant Trp387 oPGHS-1 were incubated for 30 min with 50 μM [1-^{14}C]arachidonic acid and then analyzed by thin layer chromatography and visualized by autoradiography, as described in the materials and methods. Location of the products are based on co-migration with authentic, non-radioactive standards.

and reacted for 1 min (same as in thin-layer experiments, except with non-radiolabeled substrate) and then separated by RP-HPLC. The 11-HETEs were isolated and converted to their methyl esters to be further separated by chiral HPLC. Figure 10 shows the isomer distributions of 11-HETE for the native enzyme and W387F oPGHS-1 (the 15-HETE from W387F was not isolated or separated). In both cases, 11-HETE was exclusively 11*R*-HETE. The chiral separation of W387L 11-HETE was also determined, and found to be exclusively 11*R*-HETE as well, just in much smaller quantities than W387F (Table 4).

The W387F and W387L mutants were also measured for initial oxygenation rates with various 20-carbon and 18-carbon polyunsaturated fatty acids (Table 5). The rates of cyclooxygenase activity for native oPGHS-1 with the various substrates are expressed relative to the activity with arachidonate. After arachidonic acid, the next best substrate for native oPGHS-1 was dihomo-γ-linoleic acid (20:3, also eicosatrienoic acid), at 81% of the rate with arachidonic acid. All other substrates investigated (linoleic acid, 18:2; eicosapentaenoic acid, 20:5; and eicosadienoic acid, 20:2) were oxygenated by oPGHS-1 at less than 10% of the rate with arachidonic acid. These results are very similar to those previously reported, in hPGHS-1 (49). The oxygenation rates of the mutant enzymes, W387F and W387L, with the various substrates, are expressed relative to the native oPGHS-1 with that same substrate. For example, W387F uses linoleic acid 49% as well as the native enzyme, which in turn uses this same substrate about 10% as well as it does arachidonic acid. Overall, W387F uses all tested substrates consistently, with a range of 39-50% of the native activity with

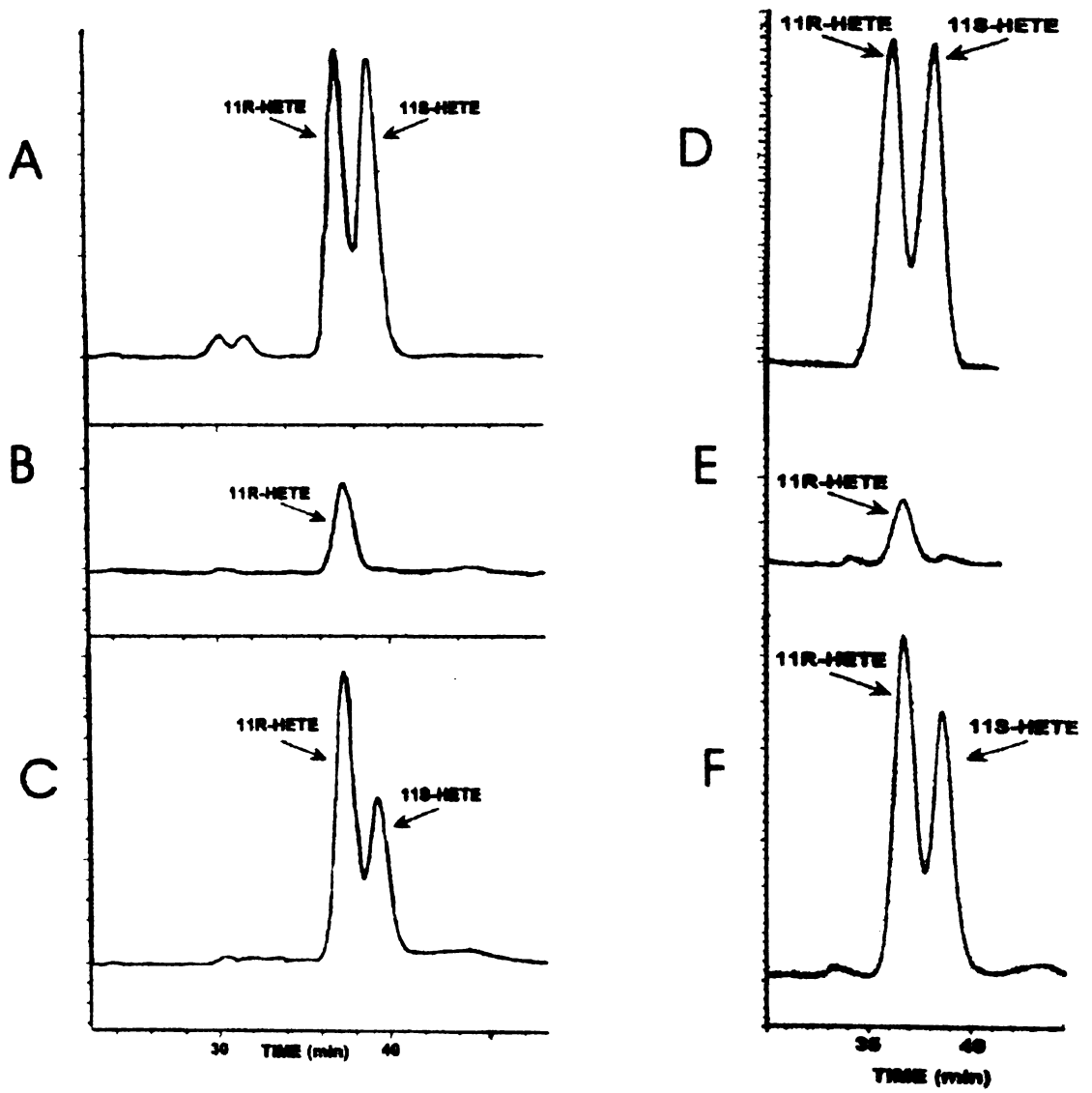

Figure 10. Chiral HPLC analysis of the methyl esters of 11-HETEs of oPGHS-1 and W387F oPGHS-1. Chiral HPLC was performed as described in the text. Absorbence was measured at 234 nm. A) 11*R/S*-HETE methyl ester standard mix; B) 11-HETE methyl ester from native oPGHS-1 incubation with arachidonic acid; C) Coinjection of 11-HETE methyl ester from native oPGHS-1 incubation with arachidonic acid and 11*R/S*-HETE methyl ester standard mix. D) 11*R/S*-HETE methyl ester standard mix; E) 11-HETE methyl ester from W387F oPGHS-1 incubation with arachidonic acid; F) Coinjection of 11-HETE methyl ester from W387F oPGHS-1 incubation with arachidonic acid and 11*R/S*-HETE methyl ester standard mix.

Table 4. Summary of chiral analysis of native oPGHS-1 and selected mutants. Based on TLC and chiral HPLC analysis.

ENZYME	% 11-HETE of total product		% 15-HETE of total product	
oPGHS-1 Native	2-3 %		1-3 %	
	100 % *R*	0 % *S*	35 % *R*	65 % *S*
W387F	35.8 %		1.3 %	
	100 % *R*	0 % *S*	ND	ND
W387L	39.2 %		1.6 %	
	100 % *R*	0 % *S*	ND	ND
F518Y	4.2 %		9.3 %	
	ND	ND	35 % *R*	65 % *S*

Table 5. Comparison of substrate specificity of oPGHS-1 and selected oPGHS-1 active site mutations. V_{MAX} values were measured as initial O_2 consumption on an oxygen electrode. Native oPGHS-1 values are expressed as a percentage of the rate seen with arachidonic acid as substrate. The mutant oPGHS-1 values are expressed as a percentage of the rate seen with the native enzyme with each individual substrate. ND, not determined.

	V_{MAX} (% 20:4)	V_{MAX} (% native activity)				
SUBSTRATE	**Native**	**W387F**	**W387L**	**M522A**	**F518Y**	**L384A**
Arachidonic acid (20:4 *n*-6)	100	44	7.8	52	38	29
Eicosatrienoic acid (20:3 *n*-6)	81	39	2.4	49	10	27
Linoleic acid (18:2 *n*-6)	9.5	49	7.0	57	22	8.1
Eicosapentaenoic acid (20:5 *n*-3)	5.4	47	1.4	ND	18	ND
Eicosadienoic acid (20:2 *n*-6)	3.3	50	0.8	25	ND	ND

those same substrates. W387L showed some differences in substrate preference, using linoleic acid and arachidonic acid with the same degree of efficiency as the native enzyme (7.0% vs 7.8%), followed then by eicosatrienoic acid (at 2.4%). Both 20:5 and 20:2 were very poor substrates for W387L.

Leu384, Phe518, and Met522 - These three sets of mutants were made in response to the results obtained with the Trp387 mutants, and substituted residues were of hydrophobic side chains of various sizes. As stated earlier, the distances of these three residues to the bound arachidonic acid substrate were recently found to be beyond the maximal distance (4 Å) for van der Waal contact, according to the crystal structure (58). But these residues are in proximity to Trp387, all within a 4-6 Å range of this residue and to each other.

All mutants constructed were able to retain some cyclooxygenase activity, as well as appreciable levels of peroxidase activity (Table 3). Western blotting indicated that all mutants were expressed at protein levels similar to that of oPGHS-1 (Figure 8B). The most detrimental mutation made was L384F, which retained only 8% of native cyclooxygenase activity with arachidonic acid (with 90% peroxidase activity retained). With the exception of L384F and one other mutant (F518Y), no other mutations constructed were bulkier in their side-chain than the native enzyme residues.

Some of the Leu384, Phe518, and Met522 mutations were measured for their K_m values with arachidonic acid as substrate, including: F518A, F518L, F518Y, M522A, and M522L (Table 3). These K_m values were all within the same range of values as the native enzyme, with a high of 20 μM for F518A. K_m values were not determined for any of the Leu384 mutants.

Product analysis of these three sets of mutants were performed using thin-layer chromatography (Figures 11, 12, and 13). Neither the Met522 mutants nor the Leu384 mutants resulted in any significant changes in the relative proportions of oxygenation products (Table 3). The substitutions to Phe518 resulted in slight increases in the overall 11-HETE and 15-HETE production. The F518Y mutant (the case where the substitution was to a slightly larger residue) resulted in the largest increase in 15-HETE formation. The isoforms of 15-HETE product with the native oPGHS-1 and F518Y were determined by separation and identification using RP-HPLC and chiral HPLC, as described before. The 15-HETEs of the native oPGHS-1 and the F518Y mutant were a mixture of approximately 65% 15*S*-HETE and 35% 15*R*-HETE (Table 4), a distribution seen previously in the native enzyme (61).

The initial oxygenation rates of selected mutants (F518Y, M522A, and L384A) were measured with alternate 20-carbon and 18-carbon substrates (Table 5), and V_{max} results are expressed similarly to those of the Trp387 mutants. M522A used all tested substrates more or less as well as the native enzyme. L384A was able to use eicosatrienoic acid similar to native oPGHS-1, but showed a marked decrease in it's ability to use linoleic acid as substrate, down to 8% from the 25-30% efficiency seen with the arachidonate and eicosatrienoic acid substrates. The F518Y mutant was not able to consistently utilize the various substrates as well as the native enzyme, with the oxygenation rates falling from 38% of native with arachidonic acid, to 22% with linoleic acid, to 18% with eicosapentaenoic acid, to 10% with eicosatrienoic acid. Unlike the native

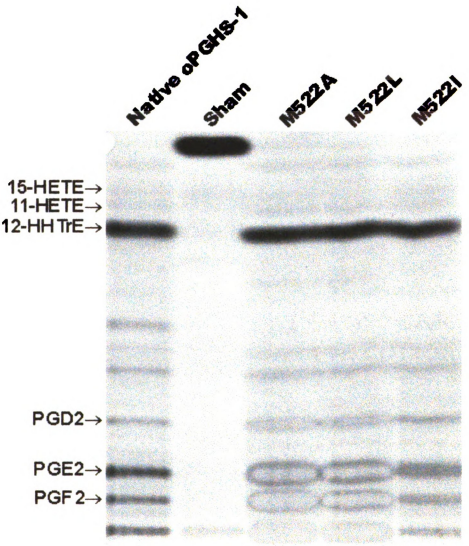

Figure 11. Thin-layer chromatograms of products formed from [1-^{14}C] arachidonic acid by native oPGHS-1 and Met522 mutants. Broken cell preparations (1 mg of protein) from COS-1 cells transfected with native or mutant Met522 oPGHS-1 were incubated for 30 min with 50 μM [1-^{14}C]arachidonic acid and then analyzed by thin layer chromatography and visualized by autoradiography, as described in the materials and methods. Location of the products are based on co-migration with authentic, non-radioactive standards.

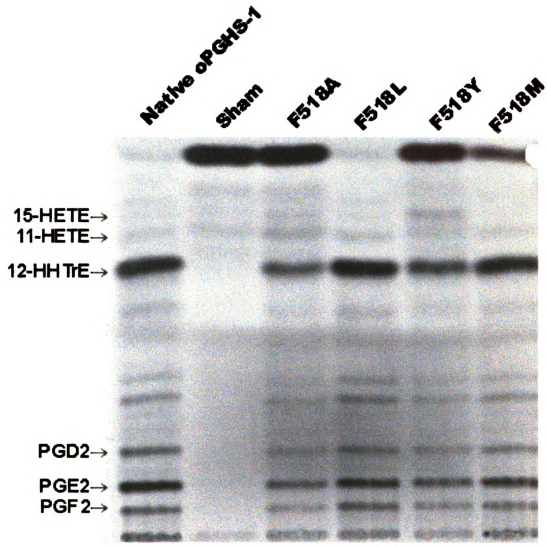

Figure 12. Thin-layer chromatograms of products formed from [1-^{14}C] arachidonic acid by native oPGHS-1 and Phe518 mutants. Broken cell preparations (1 mg of protein) from COS-1 cells transfected with native or mutant Phe518 oPGHS-1 were incubated for 30 min with 50 μM [1-^{14}C]arachidonic acid and then analyzed by thin layer chromatography and visualized by autoradiography, as described in the materials and methods. Location of the products are based on co-migration with authentic, non-radioactive standards.

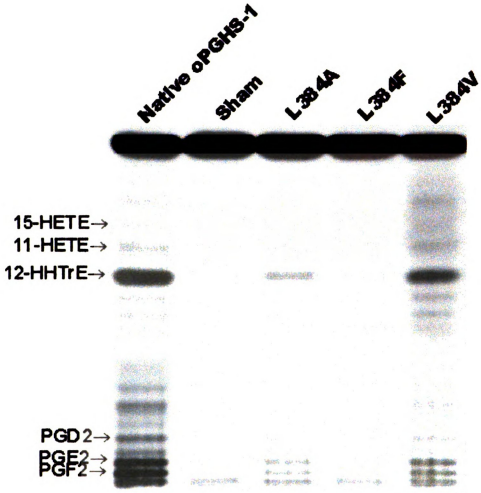

Figure 13. Thin-layer chromatograms of products formed from [1-^{14}C] arachidonic acid by native oPGHS-1 and Leu384 mutants. Broken cell preparations (1 mg of protein) from COS-1 cells transfected with native or mutant Leu384 oPGHS-1 were incubated for 1 min with 50 μM [1-^{14}C]arachidonic acid and then analyzed by thin layer chromatography and visualized by autoradiography, as described in the materials and methods. Location of the products are based on co-migration with authentic, non-radioactive standards.

enzyme, F518Y did not use eicosatrienoic acid well at all as a substrate, while the native enzyme uses this substrate well, at around 80% as efficiently as arachidonic acid.

Discussion

These sets of site-directed mutagenesis experiments were designed to examine the relative importance of selected cyclooxygenase active site residues of oPGHS-1, and the effects on substrate utilization and product formation when these residues are mutated. These results have shown that the active site residues Trp387, Met522, Phe518, and Leu384, while not essential for catalysis of substrate by oPGHS-1, still play significant roles in maintaining the overall confirmation of the oPGHS-1 cyclooxygenase active site for prostaglandin synthesis.

The most significant effects resulted in substitutions with the Trp387 residue. Polar, hydrophobic substitutions such as W387R and W387S, resulted not only in a loss of cyclooxygenase activity, but peroxidase activity as well. These residues most likely alter the proper folding of the enzyme, disrupting alignment of the residues critical for cyclooxygenase and/or peroxidase activity (e.g. Tyr385, His386, His388). The substitution of Trp387 for smaller hydrophobic residues had various effects on cyclooxygenase activity with arachidonic acid, yet all managed to retain appreciable levels of peroxidase activity. The smallest substitution, W387A, had no cyclooxygenase activity, the W387L had 8% native activity, and the largest substitution, W387F, retained 44% activity. This suggests that the Trp387 residue is not critical for catalytic activity, but is involved in proper positioning of arachidonic acid in the active site. The K_m values of W387F and W387L with arachidonic acid were not drastically altered, with at most a 10-fold increase (~25 μM) seen with W387F.

Although W387F and W387L still allow the enzyme to have functional oxygenase activity, their activity does not yield the same proportions of dihydroxy and monohydroxy products from arachidonic acid as native oPGHS-1. Around 35-40% of the total product made by W387F and W387L is the monohydroxy product 11-HpETE, while in the native oPGHS-1 this product is less than 3% of the total products formed. These mutations do not alter the stereochemical conformation of the 11-HpETE; in both the mutant and native cases the 11-HpETE is exclusively the *R*-isomer. The production of 11-HpETE in W387F and W387L is at the expense of the prostaglandin products, indicating a loss of the enzyme's ability to properly form PGG_2.

These results indicate that the large tryptophan residue is important in maintaining the close positioning of the C-9 and C-11 of arachidonic acid necessary to form the endoperoxide ring of PGG_2. The recent crystal structure of Co^{3+}-heme oPGHS-1 complexed with arachidonic acid showed that the native Trp387 residue contacts the C-11 and C-12 of arachidonic acid via the CH2 ring carbon of the indole group of tryptophan, at distances of 3.38 Å and 3.65 Å respectively. Arachidonic acid makes a substantial kink in the fatty acid chain in this C-8 to C-12 region when bound in the native active site, and it can be inferred that the residues in this area are involved in maintaining this bent conformation. The W387F and W387L are substantially smaller that the native Trp residue, and the distances from these substituted residues to bound arachidonic acid substrate are considerably further and out of range for van der Waal's contact. This presumably would preclude enzyme contact with the substrate, such that the critical endoperoxide bridge between these two carbons

cannot be completed as easily as in the native conformation. The ability of W387F and W387L to produce 40% 11-HpETE suggests that this arrangement of arachidonic acid that leads to 11-HETE production is as favorable in the mutants as arrangements that lead to PGG_2 formation. Chapter 4 further investigates and discusses the kinetics of the products formed by the native oPGHS-1 and W387F oPGHS-1. Overall, the Trp387 appears to be important in maintaining the positioning of C-11 to C-9 of arachidonic acid necessary for endoperoxide bridge formation.

The other residues in the region of the cyclooxygenase active site that were investigated were Met522, Phe518, and Leu384. While these residues are included in the first shell of residues that make up the hydrophobic cyclooxygenase active site channel, these three residues were later shown to be out of van der Waal's contact distance from the bound arachidonic acid substrate, according to the recent crystal structure. All mutations to Phe518, Met522, and Leu384 retained measurable yet varying degrees of cyclooxygenase and peroxidase activities. Mutations made to Met522 (closest to C-8 of arachidonic acid at a distance of 5.22 Å) and Phe518 (closest to the C-6 and C-8 of arachidonic acid at distances from 4.4 Å to 4.8 Å) resulted in slightly increased proportions of 11-HpETE and 15-HpETE production, but had minor effects on the K_m values for arachidonic acid.

One residue that was investigated further was F518Y, a mutation that resulted in a 3-4 fold increase in the 15-HpETE production. When this product was separated via chiral HPLC into the *R*- and *S*- isomers, the ratio of *S*:*R* was similar to the native oPGHS-1 at 65:35. This mutation, unlike the others to

Phe518, is to a slightly larger residue, a tyrosine. While the positioning of arachidonic acid may not be significantly compromised with this mutation, the decrease in the active site space close to the C-9 to C-11 region of arachidonic acid may be impeding the accessibility of the oxygen molecule addition to C-11. Therefore, while the extraction of the pro-*S* hydrogen from C-13 can still occur with F518Y, the added bulk to the outer edge of the active site does not allow as easily the addition of an O_2 molecule to C-11. The C-15 position of arachidonic acid is apparently less hindered, and could therefore still be accessible for O_2 addition, resulting in a slightly increased proportion of 15-HpETE production.

Leu384 is located nearest to the C-9 of arachidonic acid at a distance of 4.9 Å. None of the substitutions at Leu384 affected the relative proportions of oxygenated products. Of the mutations made to Leu384, the most detrimental was L384F, with the cyclooxygenase activity reduced to 8% of the native enzyme. This substitution to a bulkier residue is most likely affecting the positioning of the neighboring Tyr385, the residue critical to catalysis by abstracting the pro-*S* hydrogen of arachidonic acid. Otherwise this residue does not appear to have any critical enzymatic function or role in positioning of the substrate. Individual K_m values were not determined for this set of mutants.

The efficiency of the oPGHS-1 active site with fatty acid substrates other than arachidonic acid was investigated with selected active site mutations. The V_{max} measurements of these mutations showed that no selected mutations to Trp387, Met522, Phe518, or Leu384 increased oxygenation activity for any 20-carbon or 18-carbon fatty acids beyond that of arachidonic acid. The W387F and M522A mutants generally used all tested substrates to the same degree of

efficiency as the native oPGHS-1. L384A was able to use the substrates best oxygenated by native oPGHS-1, arachidonic acid (20:4 *n*-6) and eicosatrienoic acid (20:3 *n*-6), with similar efficiency (27-29% of native), but did not use linoleic acid (18:2 *n*-6) as substrate as well, at only 8% of the native activity with this substrate. F518Y and W387L both had diverse effects on the specificity of individual substrates, in general using substrates other than arachidonic acid poorly. The preference of substrates, even comparing all the 20-carbon to both 18-carbon fatty acids, was not conserved in any particular order with F518Y of W387L. Overall, with any of these mutants, none utilized a substrate appreciably better than it did arachidonic acid, and none of the mutations were able to use any substrate better than the native oPGHS-1.

CHAPTER 3

STUDIES TO DETERMINE KINETICS OF INDIVIDUAL OXYGENATED PRODUCTS OF NATIVE oPGHS-1 AND W387F WITH ARACHIDONIC ACID

Introduction

The first reaction of PGHS is the cyclooxygenase reaction, in which a *bis*-oxygenation converts arachidonic acid to PGG_2. The kinetics of PGHS-1 have been previously established with several substrates, with an overall K_m of around 5 μM for arachidonic acid as substrate (49, 50). While the major function of the cyclooxygenase active site is this conversion of arachidonate to PGG_2, the enzyme also exhibits lipoxygenase activity with some fatty acid substrates which results in the formation of monohydroxy products (49, 51-53). Such products from arachidonic acid substrate include 11-hydroperoxy-5*Z*,8*Z*,12*E*,14*Z*-eicosatetraenoic acid (11-HpETE) and 15-hydroperoxy-5*Z*,8*Z*,11*Z*,13*E*-eicosatetraenoic acid (15-HpETE), which are further reduced to 11-HETE and 15-HETE (60, 61). Previous studies with PGHS-2 have shown the production of 15*R*-HETE when the enzyme was pre-treated with aspirin (55). Because the mutagenic experiments to oPGHS-1 were found to alter the overall product formation of the enzyme, it was therefore necessary to clearly characterize each oxygenation product of native and the mutant W387F oPGHS-1 with arachidonic acid by determining the individual kinetic constants of these products.

Materials and Methods

Materials - Dulbecco's modified Eagle's Medium (DMEM) was purchased from Gibco. Calf serum and fetal bovine serum were from HyClone. [1-^{14}C]-Arachidonic acid was from Dupont NEN Life Science Products. 11-hydroxy-5*Z*,8*Z*,12*E*,14*Z*-eicosatetraenoic acid (11-HETE) and 15-hydroxy-5*Z*,8*Z*,11*Z*,13*E*-eicosatetraenoic acid (15-HETE) standards were purchased from Cayman Chemical Co., Inc. Bovine hemoglobin, DEAE-dextran, and chloroquine were from Sigma. Other reagents were purchased from common commercial sources.

Transfection of COS-1 cells with recombinant oPGHS-1 - COS-1 cells (ATTC CRL-1650) were grown in DMEM containing 2% fetal bovine serum and 8% calf serum, in a water-saturated 7% CO_2 atmosphere until near confluency. Cells were transfected with a pSVT7 plasmid containing cDNA coding native oPGHS-1, using a DEAE-dextran/chloroquine method previously reported (19, 27). Sham-transfected cells were also collected in a similar manner. Forty hours post-transfection the cells were harvested by scraping in ice-cold phosphate-buffered saline (PBS), centrifuged for 1200 rpm for 5 min, and resuspended in 0.1 M Tris-HCl, pH 7.5.

Characterization of arachidonate derived products by thin layer chromatography - Cell suspensions from transfected cells were disrupted by sonication and were measured at 595 nm for protein concentration using Bio-Rad Bradford protein assay reagent. Aliquots of 100 µg of protein were incubated for 1 min at 37°C

with 6.8 µg bovine hemoglobin and various concentrations of [1-^{14}C]-arachidonic acid, with and without a 5 min preincubation with 200 µM flurbiprofen. Reactions were stopped by the addition of 1.4 mL chloroform:MeOH (1:1, v:v), and then centrifuged for 10 min at 3000 rpm to remove cellular debris. Supernatants were transferred to clean tubes, and 0.6 mL chloroform and 0.32 mL 0.88% formic acid was added. The organic layer was separated by centrifugation at 3000 rpm for 5 min, extracted out into new tubes, and dried under N_2. The samples were resuspended in 50 µL chloroform and spotted onto Silica Gel 60 thin layer chromatography plates. The plates were developed twice in benzene: dioxane: acetic acid: formic acid (82:14:1:1, v/v/v/v). The products were visualized either by autoradiography using a Molecular Dynamics Storm 820 phosphorimager and ImageQuant software, or by exposure to Kodak XAR film, followed by scraping of product bands and liquid scintillation counting. Radioactive bands were identified by comparison with the authentic standards. Actual product values were calculated by subtracting out the corresponding values of samples treated with flurbiprofen.

Results

Native oPGHS-1 and W387 oPGHS-1 were expressed in transfected COS-1 cells with plasmids encoding the native or mutant oPGHS-1. Microsomal preparations, at 100 µg aliquots of total protein, were incubated with various concentrations of [1-^{14}C]arachidonic acid, in a range of 2 to 100 µM, for 1 min, and extracts of these reactions were separated by thin-layer chromatography. This range of substrate concentrations and protein allowed for approximately 25% (or less) of the substrate to be consumed at the lowest concentration of arachidonic acid (2 µM). Identical samples were incubated with 200 µM flurbiprofen as inhibitor, and these samples were run alongside the non-inhibited samples. Products were visualized by film and quantitated by liquid scintillation counting, and flurbiprofen values were subtracted out from real values of samples.

Figure 14 shows the thin-layer chromatograms of native and W387F oPGHS-1. As was also shown in Chapter 2, oPGHS-1 and W387F oPGHS-1 form the same products (PGG_2-derived products, 11-HETE, and 15-HETE), but W387F produces larger proportions of 11-HETE, at the expense of PGG_2. The lanes that contained the 200 µM flurbiprofen pre-incubations show very little, if any, conversion of [1-^{14}C]arachidonic acid.

The measurement of each of the separate products for both the native and the W387F was determined with increasing concentrations of substrate. These values were calculated as a rate (nmol of product/1 min reaction time) and both a

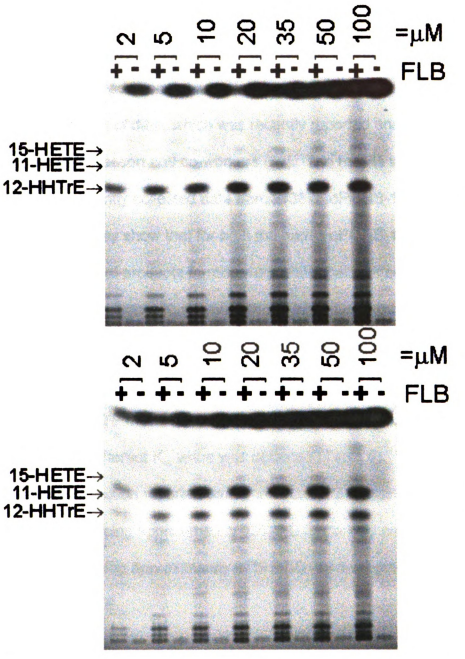

Figure 14. Thin-layer chromatograms of products formed from different concentrations of [1-^{14}C] arachidonic acid by native and W387F oPGHS-1. Broken cell preparations (100 μg)of COS-1 cells expressing A) native oPGHS-1 of B) W387F oPGHS-1 were incubated for 1 min with varying concentrations (2, 5, 10, 20, 35, 50, or 100 μM) of [1-^{14}C]arachidonic acid, with and without a 5 min preincubation with 200 μM flurbiprofen. The samples were separated by thin layer chromatography, as described in the text, and individual products were then quantitated by liquid scintillation counting. Locations of products were identified by co-migration of non-radioactive authentic standards.

V_{max} and a K_m value were determined for PGG_2-derived products and each monohydroxy fatty acid products. The values for the native oPGHS-1 were combined with additional data points collected for the native enzyme to contribute to a larger pool of date, which was recently reported and published in a related paper by Thuresson and co-workers (62). The results were compiled along with the independently collected data from W387F oPGHS-1 and are seen in Figures 15 and 16. They show that for both the native oPGHS-1 and W387F, the K_ms for the three sets of products formed were statistically different from one another (Table 6). The higher K_ms seen with the individual products of W387F correspond well with the overall K_m recorded earlier for W387F on the oxygen electrode (25 μM, see Table 3). A significant decrease in the rate with the 15-HETE of W387F made measurement of K_m difficult to accurately report, but a significantly different K_m value was obtained (Table 6). V_{max} values show that the product distribution reported earlier in Chapter 3 is maintained, with the native enzyme producing approximately 93% PGG_2-derived products, and the W387F mutant producing approximately 67% PGG_2-derived products and approximately 30% 11-HpETE.

Figure 15. Effect of arachidonic acid concentration on the formation of PGG_2, 11-HETE, and 15-HETE by native oPGHS-1. Native oPGHS-1 protein from transfected COS-1 cells was incubated at increasing concentrations of arachidonic acid at 37 °C for 1 min and analyzed by thin layer chromatography and liquid scintillation counting as indicated in the text. A) PGG_2-derived product of native oPGHS-1(●), B) 11-HpETE (○) and 15-HpETE (x) product of native oPGHS-1.

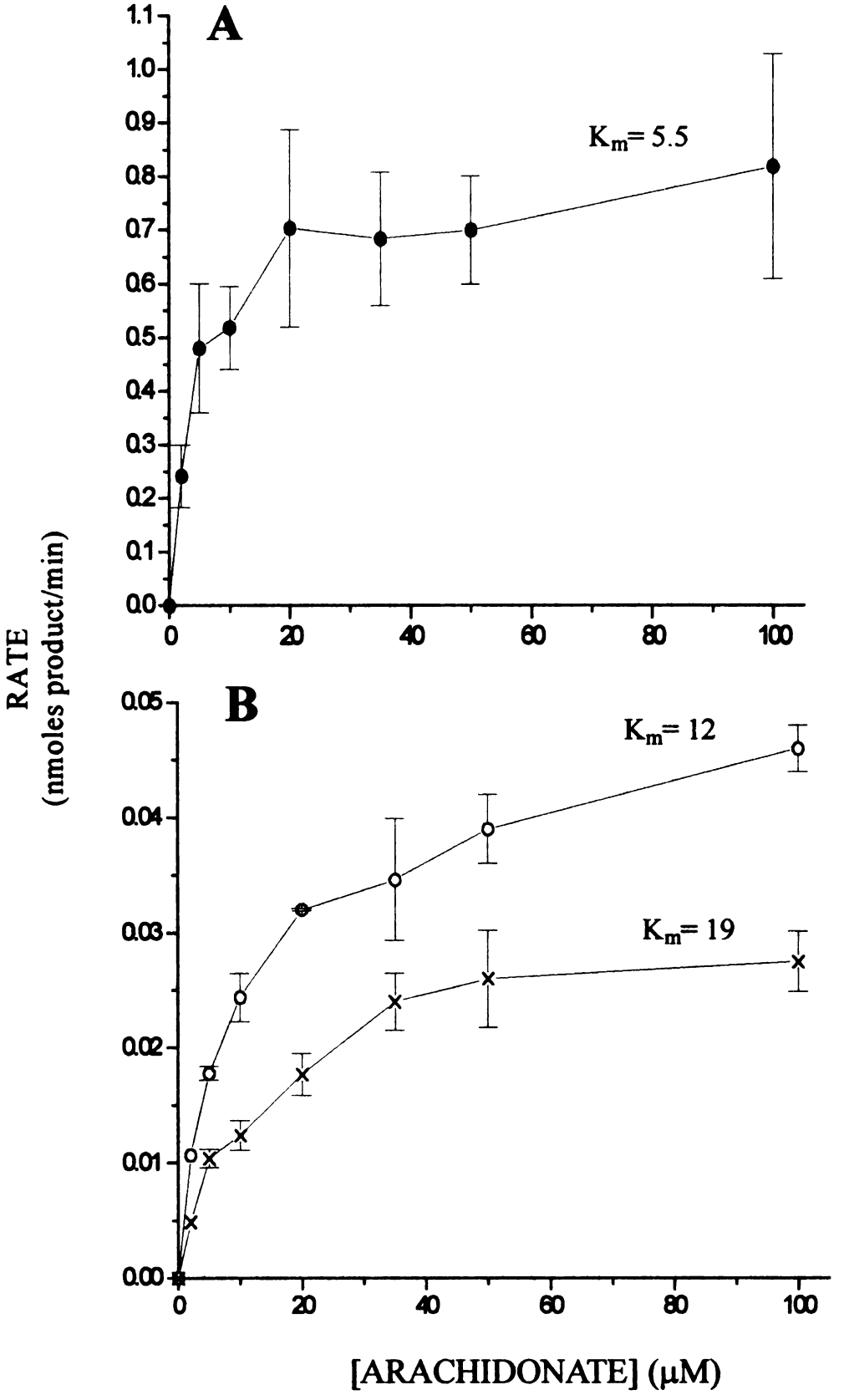

Figure 15.

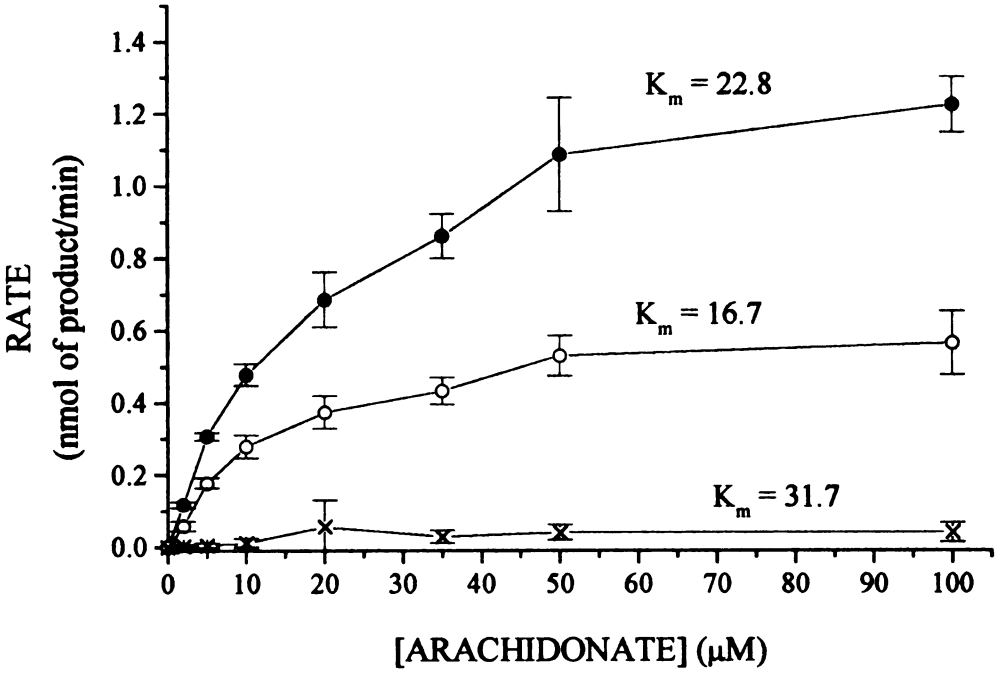

Figure 16. Effect of arachidonic acid concentration on the formation of PGG_2, 11-HETE, and 15-HETE by W387F oPGHS-1. W387F oPGHS-1 protein from transfected COS-1 cells was incubated at increasing concentrations of arachidonic acid at 37 °C for 1 min and analyzed by thin layer chromatography and liquid scintillation counting as indicated in the text. PGG_2-derived (●), 11-HpETE (○), and 15-HpETE (x) product from W387F oPGHS-1.

Table 6. Kinetic values of prostaglandin and monohydroxy acid products from arachidonic acid by native oPGHS-1 and W387F oPGHS-1. K_m and V_{MAX} values for PGG_2-derived and 11-and 15-HETE products were calculated as described in text as in Thuresson *et al.* (62). Data are from eight separate experiments for the native oPGHS-1 and from four separate experiments for W387F oPGHS-1, and are expressed ± SEM. [a]$p<0.01$ versus PGG_2 for oPGHS-1; [b]$p<0.05$ versus PGG_2 for oPGHS-1; [c]$p<0.02$ versus PGG_2 for W387F; [d]$p<0.04$ versus PGG_2 for W387F; [e]$p<0.02$ versus 11-HETE for W387F.

Products	[redacted]		[redacted]	
	K_m (μM)	V_{MAX} (nmol of product/min)	K_m (μM)	V_{MAX} (nmol of product/min)
PGG_2-derived products	5.5 ± 1.7	0.9 ± 0.05	22.8 ± 1.93	1.54 ± 0.16
11-HETE	12 ± 1.4[a]	0.04 ± 0.001	16.7 ± 4.03[c]	0.68 ± 0.13
15-HETE	19 ± 4.3[a,b]	0.03 ± 0.006	31.7 ± 7.99[d,e]	0.07 ± 0.03

Discussion

The purpose of these experiments was to better understand how the arachidonic acid substrate is binding into the cyclooxygenase active site, and especially how and why the monohydroxy product 11-HETE is formed. It was shown in Chapter 2 that the production of 11-HETE, normally a minor product (2-3% of total product converted form arachidonic acid), could be significantly increased in the W387F oPGHS-1. The question then became, which of the following was occurring: 1) was this 11-HETE production the result of the inefficiency of the mutant enzyme W387F, where the substrate was attempting, yet ultimately unable, to form PGG_2, with 11-HETE was the "fall-back" product of the enzyme, or 2) was the fate of the substrate already determined once the substrate was bound into the active site by the arrangement in which it bound. This latter explanation would then mean that the arrangement of arachidonic acid that is conductive to forming PGG_2 is less favorable in a mutant such as W387F, and the arrangement that is more conductive to forming 11-HETE is more favorable in the same mutant.

These results showed that the K_m values for the formation of PGG_2, 11-HETE, and 15-HETE were different for each product, for both the native oPGHS-1 and W387F. These results suggest that arachidonic acid assumes at least three different arrangements in the active site of oPGHS-1, which ultimately leads to the formation of PGG_2, 11-HETE, and 15-HETE. The increase in 11-HETE production with W387F then suggests that the mutant is stabilizing the conformation of arachidonic acid that would favorably make 11-HETE as product.

Conversely, the W387F mutant is less able to stabilize a conformation of arachidonic acid that would favor PGG_2 formation. Chapter 2 showed that the chirality of the products is not affected by the W387F mutation of oPGHS-1, so it is likely that the step-wise process of radical transfer and O_2 addition to the molecule is not affected by the mutation. This additional room in the active site allows for unfavorable orientation between C-9 and C-11 for endoperoxide bridge formation to be the most favored product. Overall, the substrate is not secondarily "choosing" to make 11-HETE with W387F oPGHS-1 once it binds into the cyclooxygenase active site, but this conformation of the substrate in the active site is initially more favored in the larger cyclooxygenase active site of W387F than it is with native oPGHS-1.

CHAPTER 4

STUDIES TO DETERMINE THE ROLE OF GLY533 oPGHS-1 ON CYCLOOXYGENASE ACTIVITY, AND THE EFFECTS OF A GLY533/ILE523 MUTATION IN oPGHS-1

Introduction

The Gly533 residue in oPGHS-1 was originally investigated in this laboratory using site-directed mutagenesis to determine the relative importance of those residues surrounding the aspirin-acetylation site of PGHS-1, Ser530, in substrate binding and catalysis (42). The positioning of arachidonate substrate in the cyclooxygenase active site was not fully determined at that time; in fact, it was believed that the ω-end of the substrate may have double-backed on itself in the active site, in a hairpin-like formation. The mutation G533A was found to completely lack cyclooxygenase activity, while still retaining significant peroxidase activity (54% of native) (42). It was proposed then that G533A was critical in protein chain flexibility in the active site. The loss of this flexibility with the addition of a bulkier group, even an alanine, was proposed to be hindering the ability of surrounding residues on the polypeptide chain to form a functional active site.

The recent crystal structure of oPGHS-1 complexed with arachidonic acid in the cyclooxygenase active site confirmed that the substrate is not positioned in the hairpin formation, but in an L-shaped formation, with the ω-end of the

substrate (C-12 to C-20) extending further into the catalytic domain of the enzyme, in an upper channel of the active site that is in a right angle to the lower channel (58)(Figure 6). Gly533 was determined to be within van der Waal's contact distance of the bound substrate, at 3.63 Å from C-20 (Table 1).

Gly533 is conserved in all known species of PGHS-1 and -2 (Figure 3). Studies by Rowlinson and co-workers into the G533A mutation in mouse (m) PGHS-2 measured the cyclooxygenase and peroxidase activity with several 20-carbon and 18-carbon fatty acids (63). They found that G533A mPGHS-2 retained 8% of the initial cyclooxygenase activity with arachidonic acid (20:4 *n*-6), and eventually formed 26% of the total products as the native mPGHS-2. This mutant could also utilize linolenic acid (18:3 *n*-3) as efficiently as native mPGHS-2, yet could not maintain any cyclooxygenase activity with linoleic acid (18:2 *n*-6).

Considering these results with the PGHS-2 isoform along with those seen with PGHS-1, the G533A oPGHS-1 was further analyzed in these experiments, using two additional substrates. Linolenic acid is an 18-carbon fatty acid with double bonds at C-9, C-12, and C-15, making it a ω-3 fatty acid (Figure 17). This makes it different from arachidonic acid, which is a ω-6 fatty acid (20:4 Δ5,8,11,14), and two carbons longer overall. Linoleic acid is also an 18-carbon fatty acid, but has it's double bonds only at C-9 and C-12, making it a ω-6 fatty acid, like arachidonic acid. Laneuville and co-workers' studies with these substrates in hPGHS-1 (49) showed that hydrogen abstraction by Tyr385 occurs at the ω-8 position of linoleic acid to form 9- and 13-HODEs, yet the relative abstraction occurs at the ω-5 of linolenic acid. This would seem to indicate that

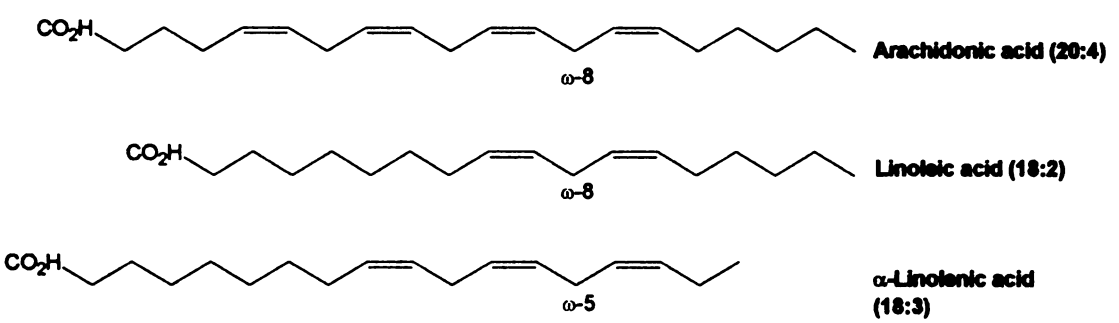

Figure 17. Structures of fatty acid substrates of oPGHS-1.

less of the terminal fatty acid segment of linolenic acid would be extending into the top channel of the active site, with a five-carbon length, than linoleic acid, with an eight-carbon length. Therefore, G533A oPGHS-1 was analyzed with these C-18 substrates as well.

Because the G533A mutant in mPGHS-2 was still able to oxygenate arachidonate acid, while the same mutant in oPGHS-1 was not, a double mutant in oPGHS-1 was constructed that would possibly mimic the active site of PGHS-2. The key core residue difference between the two isoforms is Ile523, which is the smaller Val516 in PGHS-2. The G533A/I523V double mutant was prepared, and the oxygenation rates of this mutant (and the two individual single mutations) were measured with the various substrates.

Materials and Methods

Materials - Dulbecco's modified Eagle's Medium (DMEM) was purchased from Gibco. Calf serum and fetal bovine serum were from HyClone. Arachidonic acid, linoleic acid, and α-linolenic acid, as well as all TLC standards were purchased from Cayman Chemical Co., Inc. [1-^{14}C]-Arachidonic acid (50-55 mCi/mmol) was from Dupont NEN Life Science Products. Primary antibodies used for Western blotting were raised in rabbits against purified oPGHS-1 and purified as an IgG fraction (27). Goat anti-rabbit IgG horseradish peroxidase conjugate was from BioRad. Oligonucleotides used as primers for mutagenesis and sequencing were prepared by the Michigan State University Macromolecular Structure and Sequencing Facility. Other reagents were purchased from common commercial sources.

Preparation of mutants by site directed mutagenesis - The mutants were prepared using a QuikChange site-directed mutagenesis kit (Stratagene, LaJolla, CA), with the pSVT7 oPGHS-1 plasmid as a template in polymerase chain reactions (PCR) for constructing the mutant forward and reverse primers, seen in Table 2. The PCR cycling parameters were 16 cycles of 95 °C for 30 s, 55 °C for 1 min, 68 °C for 2 min. Purification and subcloning of plasmids were essentially the same as described in the previous materials and methods section of Chapter 2.

Transfection of COS-1 cells with recombinant oPGHS-1 - COS-1 cells (ATTC CRL-1650) were grown in DMEM containing 2% fetal bovine serum and 8% calf serum, in a water-saturated 7% CO_2 atmosphere until near confluency. Cells were transfected with a pSVT7 plasmid containing cDNA coding native or mutant oPGHS-1, using a DEAE-dextran/chloroquine method previously reported (19, 27). Sham-transfected cells were also prepared in a similar manner. Forty hours post-transfection the cells were harvested by scraping in ice-cold phosphate-buffered saline (PBS), centrifuged for 1200 rpm for 5 min, and resuspended in 0.1 M Tris-HCl, pH 7.5.

Preparation of microsomes - Cells pelleted from 25-40 plates were resuspended in 5 mL of ice-cold 0.1 M Tris-HCl, pH 7.4, and disrupted by sonication. The sonicated cells were centrifuged at 10,000 rpm for 10 min at 4 °C. The resulting supernatants were ultracentrifuged at 45,000 rpm for 50 min at 4 °C using a Beckman SW50.1 swinging rotor. Microsomal membrane pellets were resuspended by homogenization in 20-30 µL of 0.1 M Tris-HCl, 1 mM phenol per culture dish. Protein concentrations were measured at 595 nm using Bio-Rad Bradford protein assay reagent.

Cyclooxygenase assays - Cyclooxygenase assays were performed by measuring the initial rate of O_2 consumption at 37 °C, using a Yellow Springs Instruments Model 5300 oxygen electrode. A standard assay mixture contained 3 mL of 0.1 M Tris-HCl, 1 mM phenol, pH 8.0, 85 µg bovine hemoglobin (as heme source), and 100 µM fatty acid substrate. Reactions were initiated by the addition of

microsomal protein (approximately 100-200 µg), in a volume of 20-80 µL, to the assay mixture, and initial rates of oxygen uptake were determined. Preincubation of 200 µM flurbiprofen inhibitor to the assay mixture determined that the oxygen consumption was due to cyclooxygenase activity.

Peroxidase assays - Peroxidase assays were performed spectrophotometrically on a Perkin-Elmer model 552A Double Beam UV-visible spectrophotometer by measuring the oxidation of 3,3,3',3'-tetramethylenephenylenediamine (TMPD) at 611 nm over time. A standard assay mixture contained 0.1 mM TMPD, 1.7 µM hematin, approximately 100 µg protein, and 0.1 M Tris-HCl, pH 8.0 to a total volume of 3 mL, and reactions were initiated by the addition of 100 µL of 0.3 mM H_2O_2.

Western blotting - Protein samples were separated on 10% polyacrylamide gels containing 0.1% SDS (SDS-PAGE) and then transferred to 0.45 µm nitrocellulose membranes using a Bio-Rad Trans-blot unit and transfer buffer containing 25 mM Tris, 192 mM glycine, and 20% methanol. Membranes were blocked for non-specific protein absorption with incubation for at least 20 min in Tris-buffered saline (20 mM Tris-Cl, 137 mM NaCl, pH 7.6) containing 0.1% Tween-20 detergent (TBS-T) and 3% non-fat dry milk. The membranes were then incubated for 2 h at 25 °C in a 1:1000 dilution of an affinity purified isozyme-specific rabbit antisera for oPGHS-1 (Gloria), followed by 3 X 10 min washes in TBS-T/1% milk. The membranes were then incubated for 1 h at 25 °C in a 1:2500 dilution of horseradish peroxidase-conjugated goat anti-rabbit IgG antibody

(BioRad), followed by 2 X 10 min washes in TBS-T/1% milk, and one 10 min wash in TBS-T alone. The proteins were visualized by chemiluminescence using Amersham ECL reagents and exposure to Kodak XAR film.

Characterization of arachidonate derived products by thin layer chromatography - Cell suspensions from transfected cells were disrupted by sonication and were measured at 595 nm for protein concentration using Bio-Rad Bradford protein assay reagent. Aliquots of 100 µg of protein were incubated for 1 min at 37 °C with 6.8 µg bovine hemoglobin and a high concentration (50-100 µM) of [1-^{14}C]-arachidonic acid. Reactions were stopped by the addition of 1.4 mL chloroform:MeOH (1:1, v/v), and then centrifuged for 10 min at 3000 rpm to remove cellular debris. Supernatants were transferred to clean tubes, and 0.6 mL chloroform and 0.32 mL 0.88% formic acid was added. The organic layer was separated by centrifugation at 3000 rpm for 5 min, extracted out into new tubes, and dried under N_2. The samples were resuspended in 50 µL chloroform and spotted onto Silica Gel 60 thin layer chromatography plates. The plates were developed twice in benzene: dioxane: acetic acid: formic acid (82:14:1:1, v/v/v/v). The products were visualized by exposure to Kodak XAR film, followed by scraping of product bands and liquid scintillation counting. Radioactive bands were identified by comparison with the authentic standards. Actual product values were calculated by subtracting out the corresponding values of sham-transfected samples.

Results

Native oPGHS-1 and all mutants were transiently expressed in COS-1 cells and microsomal membrane fractions of each were assayed for initial cyclooxygenase activity (V_{max}), using 100 μM arachidonic acid as substrate, and peroxidase activity, using H_2O_2 and TMPD as co-substrates. The individual products of some of the cyclooxygenase-active of these mutants were separated by thin-layer chromatography and quantified by densitometry. In all cases, sham-transfected cells were analyzed for activity alongside cells transfected with native oPGHS-1 or the various oPGHS-1 mutants. The results are summarized in Table 7, and the data shown are normalized to the relative activities of the native enzyme.

The G533 residue of oPGHS-1 is located at the end of the top channel of the cyclooxygenase active site, and the crystal structure complexed with arachidonic acid showed that the Cα of the residue lies 3.63 Å from the C-20 of arachidonic acid. The G533A mutant in oPGHS-1 was originally constructed in an effort to define the important residues surrounding Ser530, the site of aspirin acetylation (42). That previous investigation showed that the G533A mutant had no cyclooxygenase activity, yet retained peroxidase activity. This present study continued on with these findings and investigated the ability of the G533A to utilize either linoleic acid or linolenic acid. Surprisingly, neither the *n*-6 (linoleic acid) nor the *n*-3 (linoleic acid) fatty acid was able to be oxygenated by this mutant, and it was confirmed that this mutant still had 85% of native peroxidase activity (Table 7). As stated earlier, the G533A mPGHS-2 was able to maintain

Table 7. Kinetic properties and product analysis for Gly533 and Ile523 oPGHS-1 mutants with arachidonic acid substrate. Measurements were made as described in text, and similarly to Table 3 in Chapter 2.

ENZYME	CYCLOOXYGENASE V_{MAX} (% native)	PEROXIDASE (% native)	11-HETE (% of total products)	15-HETE (% of total products)
Native oPGHS-1	100	100	1.9	1.2
Sham	0	0	–	–
G533A	0	85	–	–
I523V	32	57	2.0	1.7
G533A/ I523V	0	53	–	–

partial (8% of native) initial cyclooxygenase activity with arachidonic acid (63). In addition, this mPGHS-2 mutant was able to oxygenate linolenic acid and stearidonic acid, both *n*-3 fatty acids, as efficiently as the native enzyme, yet was unable to oxygenate linolenic acid, an *n*-6 fatty acid.

In response to these results, a double mutant in oPGHS-1 was constructed, G533A/I523V, to see if mPGHS-2-like results could be observed. While a single mutation in oPGHS-1 of Ile523 to a valine (the corresponding residue in PGHS-2) was still able to oxygenate arachidonic acid (32% of initial native cyclooxygenase activity), G533A/I523V was not able to retain any cyclooxygenase activity with either arachidonic acid, linoleic acid, or linolenic acid at high (100 μM) concentrations (Table 7). Peroxidase activity was maintained in all mutants. Interestingly, when the products were separated via thin-layer chromatography, the single mutation, I523V, was shown to have total oxygenated products closer to 75% of native oPGHS-1, and with similar distribution of products (96% PGG_2-derived products, 2% 11-HETE, and 2% 15-HETE). Western blot analysis of all three mutations in oPGHS-1 (G533A, I523V, and G533A/I523V) maintained that protein expression levels were compatible to native oPGHS-1 (data not shown).

Discussion

This set of experiments was performed to determine the extent of the effects of a mutation to Gly533. This residue lies at the end of the cyclooxygenase active site upper channel, with the main chain carbon of the glycine located 3.63 Å from the C-20 of bound arachidonic acid. The G533A mutation was unable to oxygenate arachidonic acid, but retained the peroxidase activity of the enzyme. It can therefore be interpreted that the added bulk of a methyl group to the end of the cyclooxygenase active site does not allow for the full extension of the methyl end of arachidonic acid into the active site. In oPGHS-1, arachidonic acid is bound into the active site at the carboxyl end at the end of the active site, by Arg120. Assuming that the substrate is even getting bound into the active site, the presence of the alanine group at the end of the active site is probably keeping the rest of the C-9 to C-20 portion of arachidonic acid from positioning correctly into the upper active site channel, most critically where the C-13 pro-*S* hydrogen must be aligned properly with Tyr385 for hydrogen abstraction for the first step in conversion to PGG_2. This would explain the complete lack of cyclooxygenase activity in G533A oPGHS-1.

Two 18-carbon fatty acids were also tested for oxygenation with this mutant. Linoleic acid (18:2 *n*-6) is a shorter substrate, with two less carbons than arachidonic acid, but the hydrogen abstraction of this substrate by PGHS-1 takes place at the C-11, which is the ω-8 position of the fatty acid, the same as the C-13 of arachidonic acid. This would suggest that the same length of fatty acid

chain would need to extend into this upper portion of the active site. As somewhat expected then, the G533A was unable to oxygenate linoleic acid.

A second fatty acid, α-linolenic acid (18:3 *n*-3) was also tested with G533A. Unlike 20:4 and 18:2, linolenic acid is converted to it's main product, 12-HOTrE, by the abstraction of the hydrogen at the ω-5 position (C-14), not the ω-8. Therefore, it was predicted that this substrate would not extend as far into the upper channel, reducing the chance that the substitution of alanine at Gly533 would hinder positioning and subsequent oxygenation of this substrate. However, G533A was shown to lack any cyclooxygenase activity with this substrate as well. One explanation for this result is that the methyl end of α-linolenic acid may be in a very elongated conformation in the upper portion of the active site, and yet still properly align the C-14 with Tyr385 for hydrogen abstraction. This would mean that four carbons of α-linolenic acid would be taking up the same length of the upper channel as the seven carbons of linoleic acid or arachidonic acid. Another possible explanation is that the mutation of a glycine to an alanine in this position is creating disruptions to other residues in this area of the active site. This region of the active site of oPGHS-1 has several large hydrophobic residues, including Phe205, Phe209,Leu534, Phe381, and Ile377. If the substitution to an alanine impeded on the overall proper folding or orientation of other residues in this area of the active site channel, it is possible that the hindrance to substrate could be occurring well before the area where the C-20 normally is positioned. This could explain the inability of even the α-linolenic acid to be oxygenated by G533A.

Both of these explanations are further complicated, however, by the observations reported by Rowlinson and co-workers with the same mutated residue in mPGHS-2 (63). They reported that G533A mPGHS-2 could still maintain some cyclooxygenase activity with arachidonic acid, yet could not oxygenate linoleic acid, the other substrate where the hydrogen abstraction takes place at the ω-8 position. Also, they found that in fatty acids where the ω-5 hydrogen was abstracted, such as α-linolenic acid and also stearidonic acid, this mutation in mPGHS-2 had little effect on cyclooxygenase activity. In fact, a substitution as large as a leucine at position 533 still permitted oxygenation of these fatty acids, but at a reduced rate.

The question then posed was why PGHS-2 was able to oxygenate α-linolenic acid, while oPGHS-1 was not. One major difference between the two isoforms of PGHS is that the carboxyl end of substrates must bind to the Arg120 of the PGHS-1 active site, but this substrate binding at the Arg106 of PGHS-2 is not necessary for enzyme activity. The other major difference between the isoforms is that PGHS-2 has a larger active site than PGHS-1, due in a significant degree to the substitution of a Val509 in PGHS-2 versus the larger Ile523 in PGHS-1. Accordingly, a G533A/I523V double mutation was prepared in oPGHS-1 to determine if this substitution would render the PGHS-1 active site to be more like that of PGHS-2. However, this double mutation was still unable to oxygenate arachidonic acid, linoleic acid, or α-linolenic acid. The I523V single mutation did not contribute to this loss of activity; this active site mutation still retained an appreciable amount of native cyclooxygenase initial activity with all tested substrates, and had a high percentage (upwards of 75%) of the total

products formed, and in the same proportions as the native enzyme. According to the complexed oPGHS-1/arachidonic acid crystal structure, Ile523 lies on the outer edge of the lower active site channel, with van der Waal contact distances of 3.31 Å to C-5, 3.44 Å to C-6, and 3.8 Å to C-2 of arachidonic acid, suggestive of a more crucial role in substrate binding and/or positioning, but this was not observed in these studies. Previously, changes of the Ile523 site to a valine (combined with a H513R mutation) in PGHS-1 have shown to render the active site sensitive to PGHS-2-selective inhibitors (48), but it appears that this 523/509 site may be more significant in it's ability to enhance inhibitor selectivity than it is in being crucial to substrate binding and proper alignment of substrate in the active site. These results indicate that the difference between the PGHS-1 and PGHS-2 active sites is not limited to this core 523/509 residue, but probably a combination of several residues that contribute to an overall looser fit of the substrate into the PGHS-2 active site. How PGHS-2 is able to oxygenate fatty acids with apparently less need of substrate constraints in the active site is unknown, and will require further investigation.

CONCLUSIONS

The PGHS-1 cyclooxygenase active site is a long L-shaped channel of primarily hydrophobic residues that is designed to bind a variety of fatty acid substrates for catalytic conversion to dihydroxy and monohydroxy products. The most critical residues in this channel are the Tyr385, which is necessary for the pro S-hydrogen abstraction from the substrate, and the Arg120, necessary for the binding of the carboxyl end of the substrate to the mouth of the active site. These sets of experiments studied the relative effects of several other active site residues, including those located at the bend in the active site (Trp387, Met522, Phe518, and Leu384), as well as one located at the far end of the upper channel (Gly533), and another that is one of the few differences between PGHS-1 and PGHS-2 active sites (Ile523). Overall, it was shown that mutations to these residues have a range of effects on cyclooxygenase activity and product formation with arachidonic acid as the substrate.

One of the most interesting sets of mutations was to Trp387. This residue has direct contact to bound arachidonic substrate, and is located in the region where the endoperoxide bridge formation must occur for successful conversion to PGG_2. Non-hydrophobic residues were not tolerated at this site, but the larger the hydrophobic residue substituted for Trp, the better the overall cyclooxygenase activity of that mutant. This suggested that this residue is involved in maintaining the spacial constraints necessary in the active site for PGG_2 formation. The product analysis of these mutated enzymes showed the formation of high levels of the monohydroxy product 11-HpETE, which is normally a minor (2-3%) product

formed by the native enzyme. The K_ms of the individual products formed by both the native enzyme and the mutant W387F were determined as well, and it was shown that the K_ms were different for each product, suggesting that the formation of such products can be considered separate, predetermined reactions. Additional inhibitor studies of the native oPGHS-1 were able to show that the enzyme is probably allowing at least three separate arrangements of arachidonic acid in the active site, all of which will yield a separate product (62). The mutation of Trp387 to Phe or Leu residues seems more often to allow the arachidonic conformation that will ultimately result in the formation of 11-HETE than seen with the native enzyme. This is most likely due to the lack of constraint in the substrate that is needed for the orientation of the C-11 and C-9 to each other for endoperoxide bridge formation using the O_2 that is already been bound at the C-11 of arachidonic acid.

Other sets of mutations to this same general area of the active site were less significant in their effects on either the cyclooxygenase activity, or the resulting products formed. The most damaging mutation was made to Leu384; by substituting a larger Phe, the activity was significantly decreased, probably due to the disruption of the neighboring Tyr385 residue that must be positioned at the C-13 of the bound arachidonic acid. Other mutations to Leu384, as well as to Met522 and Phe518, had various effects on initial rates of oxygenation with arachidonic acid and other fatty acid substrates, but overall they are not critical to enzymatic activity. Generally, it seems that each first-shell hydrophobic residue is contributing to some degree to maintaining the overall integrity of the active site by positioning the arachidonic acid. It is interesting to note that the residues that

have recently been shown to have actual van der Waal contact with the substrate are the ones that have the greatest effect on the activity and product formation, which fits nicely with the results seen in these studies.

The studies of the Gly533 were interesting in that any mutation to this methyl end contact residue resulted in complete loss of cyclooxygenase activity, regardless of the fatty acid substrate tested. This residue does come within van der Waals contact of the terminal carbon of arachidonic acid substrate, so it is possible that the substitution of a larger residue here results in the misalignment of the substrate in the active site, where the C-13 of arachidonic acid or linoleic acid is not properly positioned to Tyr385. What is less clear is why a substrate such as α-linolenic acid is also completely unable to be oxygenated by G533A oPGHS-1. A crystal structure of the oPGHS-1 active site with a ω-3 fatty acid such as α-linolenic acid may be able to eventually explain these findings, by showing how the ω-end of this type of substrate is positioned in the upper channel of the active site. The studies published of the same mutation to Gly533 in mPGHS-2 showed that this isoform was able to tolerate conservative substitutions to this region. The combination of these results contributes to the observations that have been made about the differences between PGHS-1 and PGHS-2 active sites. Overall, the PGHS-2 active site is larger in space, and has been shown to tolerate mutations to the active site better than PGHS-1. Experiments to G533A oPGHS-1 where the additional mutation of Ile523 to a smaller Val was made showed that this one residue alone is not responsible for the G533A mPGHS-2 activity observed in the previous study. It appears that the differences between PGHS-1 and PGHS-2 active sites is not limited to one

residue, but probably a combination of several residues. Mutational studies into combinations of possible relevant cyclooxygenase active site residues is currently underway in this laboratory.

The results of these studies have contributed to a clearer understanding of the oPGHS-1 active site, and have helped support not only the model of the conversion of arachidonic acid to PGG_2, but also the structural data obtained from the crystal structure of the cyclooxygenase active site.

REFERENCES

1. Fitzpatrick, F. A. and Smith, W. L. (1996) in *Biochemistry of Lipids, Lipoproteins and Membranes* (Vance, D. E. and Vance, J. E., eds.), pp. 283-308, Elsevier Science B.V., Amsterdam.

2. Smith, W. L. and Marnett, L. J. (1991) *Biochim. Biophys. Acta* **1083**, 1-17.

3. DeWitt, D. L. (1991) *Biochim. Biophys. Acta* **1083**, 121-134.

4. Hamberg, M. (1972) *Biochem. Biophys. Res. Commun.* **49**, 720-726.

5. Smith, W. L. and DeWitt, D. L. (1995) *Semin. Nephrol.* **15**, 179-194.

6. DeWitt, D. L. (1999) *Mol. Pharmacol.* **4**, 625-631.

7. Smith, W. L. (1992) *Am. J. Physiol.* **263**, F181 -F191.

8. Clark, J. D., Schievella, A. R., Nalefski, E. A., and Lin, L.-L. (1995) *J. Lipid Mediat. Cell Signal.* **12**, 83-117.

9. Murakami, M., Shimbara, S., Kambe, T., Kuwata, H., Winstead, M. V., Tischfield, J. A., and Kudo, I. (1998) *J. Biol. Chem.* **273**, 14411-14423.

10. Nalefski, E. A., Sultzman, L. A., Martin, D. M., Kriz, R. W., Towler, P. S., Knopf, J. L., and Clark, J. D. (1994) *J. Biol. Chem.* **269**, 18239-18249.

11. Schievella, A. R., Regier, M. K., Smith W. L., and Lin, L.-L. (1995) *J. Biol. Chem.* **270**, 30749-30754.

12. Lin, L.-L., Wartmann, M., Lin, A. Y., Knopf, J. L., Seth, A., and Davis, R. J. (1993) *Cell* **72**, 269-278.

13. Tazawa, R., Xu, X. M., Wu, K. K., and Wang, L. H. (1994) *Biochem. Biophys. Res. Commun.* **203**, 190-199.

14. Otto, J. C. and Smith, W. L. (1995) *J. Lipid Mediat. Cell Signal.* **12**, 139-156.

15. Hemler, M., Lands, W. E. M., and Smith, W. L. (1976) *J. Biol. Chem.* **251**, 5575-5579.

16. Miyamoto, T., Ogino, N., Yamamoto, S., and Hiyaishi, O. (1976) *J. Biol. Chem.* **251**, 2629-2636.

17. van der Ouderaa, F. J., Buytenhek, M., Nugteren, D. H., and van Dorp, D. A. (1997) *Biochim. Biophys. Acta* **487**, 315-331.

18. DeWitt, D. L. and Smith, W. L. (1988) *Proc. Natl. Acad. Sci. USA* **85**, 1212-1416.

19. DeWitt, D. L., El-Harith, E. A., Kraemer, S.A., Andrews, M. J., Yao, E. F., Armstrong, R. L., and Smith, W. L. (1990) *J. Biol. Chem.* **265**, 5192-5198.

20. Yokoyama, C. and Tanabe, T. (1989) *Biochem. Biophys. Res. Commun.* **165**, 888-894.

21. Feng, L., Sun, W., Xia, Y., Tang, W. W., Chanmugam, P., Soyoola, E., Wilson, C. B., and Hwang, D. (1993) *Arch. Biochem. Biophys.* **307**, 361-368.

22. Hla, T. and Neilson, K. (1992) *Proc. Natl. Acad. Sci. USA* **89**, 7384-7388.

23. Kujubu, D. A., Fletcher, B. S., Varnum, B. C., Lim, R. W., and Herschman, H. R. (1991) *J. Biol. Chem.* **266**, 12866-12872.

24. Xie, W., Chipman, J. G., Robertson, D. L., Erikson, R. L., and Simmons, D. L. (1991) *Proc. Natl. Acad. Sci. USA* **88**, 2692-2696.

25. Otto, J. C., DeWitt, D. L., and Smith, W. L. (1993) *J. Biol. Chem.* **268**, 18234-18242.

26. Regier, M. K., DeWitt, D. L., Schindler, M. S., and Smith, W. L. (1993) *Arch. Biochem. Biophys.* **301**, 439-444.

27. Otto, J. C. and Smith, W. L. (1994) *J. Biol. Chem.* **269**, 19868-19875.

28. Morita, I.., Schindler, M., Regier, M. K., Otto, J. C. , Hori, T., DeWitt, D. L., and Smith, W. L. (1995) *J. Biol. Chem.* **270**, 10902-10908.

29. Spencer, A. G., Woods, J. W., Arakawa, T., Singer, I. I. , and Smith, W. L. (1998) *J. Biol. Chem.* **273**, 9886-9893.

30. Picot, D., Loll, P. J. and Garavito, R. M. (1994) *Nature* **367**, 243-249.

31. Otto, J. C. and Smith, W. L. (1996) *J. Biol. Chem.* **271**, 9906-9910.

32. Luong, C., Miller, A. Barnett, J., Chow, J., Ramesha, C., and Browner, M. F. (1996) *Nat. Struct. Biol.* **3**, 927-933.

33. Kurumbail, R. G., Stevens, A. M., Gierse, J. K., McDonald, J. J., Stegeman, R. A., Pak, J. Y., Gildehaus, D., Miyashiro, J. M., Penning, T. D., Seibert, K., Isakson, P. C., and Stallings, W. C. (1996) *Nature* **384**, 644-648.

34. Malkowski, M. G., Theisen, M. J., Scharmen, A., and Garavito, R. M. (2000) *J. Biol. Chem.* (**in press**).

35. Karthein, R., Dietz, R., Nastainczyk, W., and Ruf, H. H. (1988) *Eur. J. Biochem.* **171**, 313-320.

36. Shimokawa, T., Kulmacz, R. J., DeWitt, D. L., and Smith, W. L. (1990) *J. Biol. Chem.* **265**, 200073-20076.

37. van der Ouderaa, F. J., Buytenhek, M., Slikkerveer, F. J., and van Dorp, D. A. (1979) *Biochim. Biophys. Acta* **572**, 29-42.

38. Ruf, H. H., Schuhn, D., and Nastainczyk, W. (1984) *FEBS Lett.* **165**, 293-296.

39. Shimokawa, T. and Smith, W. L. (1991) *J. Biol. Chem.* **266**, 6168-6173.

40. Landino, L. M., Crews, B. C., Gierse, J. K., Hauser, S. D., and Marnett, L. J. (1997) *J. Biol. Chem.* **272**, 21565-21574.

41. Roth, G. J., Machuga, E. T., and Ozols, J. (1983) *Biochemistry* **22**, 4672-4675.

42. Shimokawa, T. and Smith, W. L. (1992) *J. Biol. Chem.* **267**, 12387-12392.

43. Mancini, J. A., Riendeau, D., Falgueyret, J.-P., Vickers, P. J., and O'Neill, G. P. (1995) *J. Biol. Chem.* **270**, 29372-29377.

44. Bhattacharyya, D. K., Lecomte, M., Rieke, C. J., Garavito, R. M., and Smith, W. L. (1996) *J. Biol. Chem.* **271**, 2179-2184.

45. Rieke, C. J., Mulichak, A. M., Garavito, R. M., and Smith, W. L. (1999) *J. Biol Chem.* **274**, 17109-17114.

46. Gierse, J. K., McDonald, J. J., Hauser, S. D., Rangwala, S. H., Koboldt, C. M., and Seibert, K. (1996) *J. Biol. Chem.* **271**, 15810-15814.

47. Guo, Q., Wang, L.-H., Ruan, K.-H., and Kulmacz, R. J. (1996) *J. Biol. Chem.* **271**, 19134-19139.

48. Wong, E., Bayly, C., Waterman, H. L., Riendeau, D., and Mancini, J. A. (1997) *J. Biol. Chem.* **272**, 9280-9286.

49. Laneuville, O., Breuer, D. K., Xu, N., Huang, Z. H., Gage, D. A., Watson, J. T., Lagarde, M., DeWitt, D. L., and Smith, W. L. (1995) *J. Biol. Chem.* **270**, 19330-19336.

50. Meade, E. A., Smith, W. L., and DeWitt, D. L. (1993) *J. Biol. Chem.* **268**, 6610-6614.

51. Hamberg, M. and Samuelsson, B. (1967) *J. Biol. Chem.* **242**, 5336-5343.

52. Kulmacz, R. J., Pendleton, R. B., and Lands, W. E. M. (1994) *J. Biol. Chem.* **269**, 5527-5536.

53. Hamberg, M. and Samuelsson, B. (1967) *J. Biol. Chem.* **242**, 5344-5354.

54. Lecomte, M., Laneuville, O, Ji, C., DeWitt, D. L., and Smith, W. L. (1994) *J. Biol. Chem.* **269**, 13207-1321.

55. Holtzman, M. J., Turk, J., and Shornick, L. P. (1992) *J. Biol. Chem.* **267**, 21438-21445.

56. Mancini, J. A., O'Neill, G. P., Bayly, C., and Vickers, P. J. (1994) *FEBS Lett.* **342**, 33-37.

57. Hsi, L.C., Tsai, A., Kulmacz, R. J., English, D. G., Siefker, A. O., Otto, J. C., and Smith, W.L. (1993) *J. Lipid. Med.* **6**, 131-138.

58. Malkowski, M.G., Ginell, S., Smith, W.L., and Garavito, R.M. (2000) *Science*, submitted.

59. Laneuville, O., Breuer, D. K., DeWitt, D. L., Hla, T., Funk, C.D., and Smith, W.L. (1994) *J. Pharm. Exp. Therap.* **271**, 927-934.

60. Hecker, M., Ullrich, V., Fischer, C., and Meese, C. O. (1987) *Eur. J. Biochem.* **169**, 113-123.

61. Xiao, G., Tsai, A. L., Palmer, G., Boyar, W. C., Marshall, P. J., and Kulmacz, R. J. (1997) *Biochemistry* **36**, 1836-1845.

62. Thuresson, E. D., Lakkides, K. M., and Smith, W. L. (2000) *J. Biol. Chem.* **275**, 8501-8507.

63. Rowlinson, S. W., Crews, B.C., Lanzo, C. A., and Marnett, L. J. (1999) *J. Biol. Chem.* **274**, 23305-23310.